Efficient Synthesis of Covalent Organic Frameworks in Supercritical Carbon Dioxide and their Application in Iodine Capture

Hai Jiang,[‡,1] Shenglin Wang,[‡,1] Bin Zheng,[2] Xiaofang Su,[1] Muhammad Naveed Javed*[,1] Hui Hu,*[,1] Huanjun Xu,[3] and Yanan Gao*[,1]

[1] Key Laboratory of Advanced Materials of Tropical Island Resources, Ministry of Education, School of Chemistry and Chemical Engineering, Hainan University, No 58, Renmin Avenue, Haikou 570228, China.

[2] Hainan Nuclear Power Co., Ltd, Haikou 570125, China.

[3] School of Science, Qiongtai Normal University, Haikou 571100, China.

Corresponding: naveedjaved@hainanu.edu.cn (M.N. Javed); hhu@hainanu.edu.cn (H. Hu); ygao@hainanu.edu.cn (Y. Gao)

Table of Contents

Instrumentation and materials

All reagents were obtained commercially from Tianjin Hiensopude Technology Co., Ltd., Shanghai Bide Pharmaceutical Technology Co., Ltd., Haikou Kecheng Laibo Technology Co., Ltd., Haikou Tonglixing Chemical Raw Materials Co., Ltd., and Utop Technology Suzhou Co., Ltd., and were used as received without further purification. Fourier-transform infrared spectroscopy (FT-IR) spectra were recorded on a JASCO FT/IT-6800 Fourier Transform infrared spectrometer. Ultrasonication was carried out using a KQ-500DE ultrasonic cleaner (Kunshan Ultrasonic Instrument Co., Ltd.). Powder X-ray diffraction (PXRD) analysis was conducted on a Rigaku X-ray diffractometer XRD-MiniFlex600 with Cu Kα radiation (λ = 1.542 Å), a 2θ range of 2-30º, a scan rate of 10º min^{-1}, and slit settings of 1/5º (incidence) and 12.075 mm (receiving). The specific surface area and pore size distribution of the COF samples were determined by nitrogen adsorption-desorption measurements using the BET method. The analysis was performed on a Autosorb IQ2 gas adsorption analyzer (Quantachrome Instruments). Prior to measurement, approximately 20-50 mg of sample was first vacuum-dried at ambient temperature for 12 hours to remove residual solvents, then transferred to a BET analysis tube and further degassed under vacuum at 120 ℃ for an additional 12 hours. The adsorption-desorption isotherms were measured at 77 K (-196 ℃), and pore size distributions were calculated using both the slit-pore model and non-local density functional theory (NLDFT) equilibrium model. UV-visible spectroscopy (UV-Vis) measurements were recorded on a JASCO V-770 spectrophotometer using quartz cuvettes, with methanol desorption tests (200-800 nm). The adsorption of iodine by COFs in n-hexane test ranges from 300-800 nm, the test adopts absorption mode, with UV/visible light bandwidth of 5.0 nm, scanning speed of 400 nm min^{-1}.

Synthetic of $scCO_2$-COFs

General method for the synthesis of $scCO_2$-COFs

The respective amine (0.075 mmol) and aldehyde (0.05 mmol) were added to a 5 mL small-mouth glass vial. Acetic acid (1 mL, 6.0 M) was introduced, and the mixture was sonicated for 2 minutes to form a homogeneous suspension. The vial opening was covered with ordinary filter paper, secured with a rubber band. A small hole was perforated in the filter paper using a syringe needle to allow pressure equilibration. The vial was placed inside a supercritical CO_2 reactor. The reaction proceeded at 85 °C and 8.5 MPa for 2 hours under supercritical CO_2. After cooling, the vial was removed, and the crude product was washed with THF. The product was transferred to a Soxhlet extractor and purified with THF for 12 hours. The purified powder was collected by filtration and dried at 100 °C under reduced pressure for 12 hours, yielding the final product.

Synthesis of $scCO_2$-COF-BATH-AP

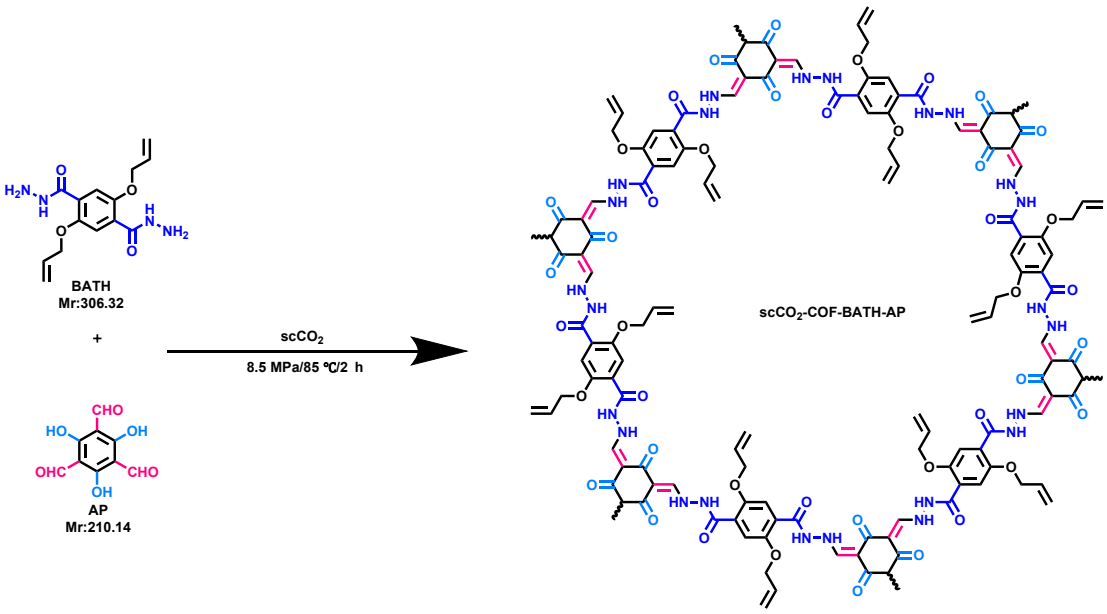

Traditional solvothermal method: The COF-BATH-AP was synthesized in 3 days at 120 °C by using 1,4-dioxane/mesitylene as solvent. The reported yield of the COF was 75 % [1].

The $scCO_2$ method: The $scCO_2$-COF-BATH-AP was obtained in $scCO_2$ according to the general method in 2 hours. The yield of $scCO_2$-COF-BATH-AP is 86.7%.

Synthesis of $scCO_2$-COF-TAPB-DMTA

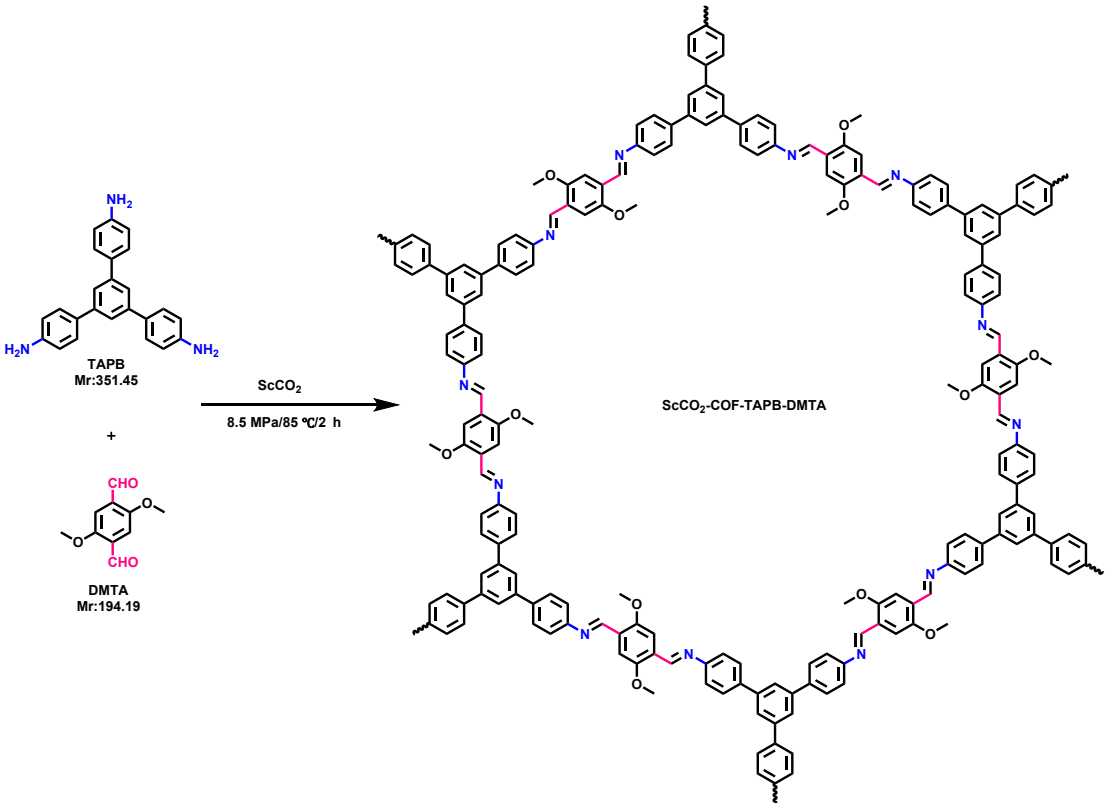

Traditional solvothermal method: COF-TAPB-DMTA was synthesized in 3 days at 120 °C by using 1,4-dioxane/mesitylene as the solvent. The reported yield of the COF was 81% [2].

The $scCO_2$ method: The $scCO_2$-COF-TAPB-DMTA was obtained in $scCO_2$ according to the general method in 2 hours. The yield of the $scCO_2$-COF-TAPB-DMTA is 64.61%.

Synthesis of $scCO_2$-COF-TAPT-DMTA

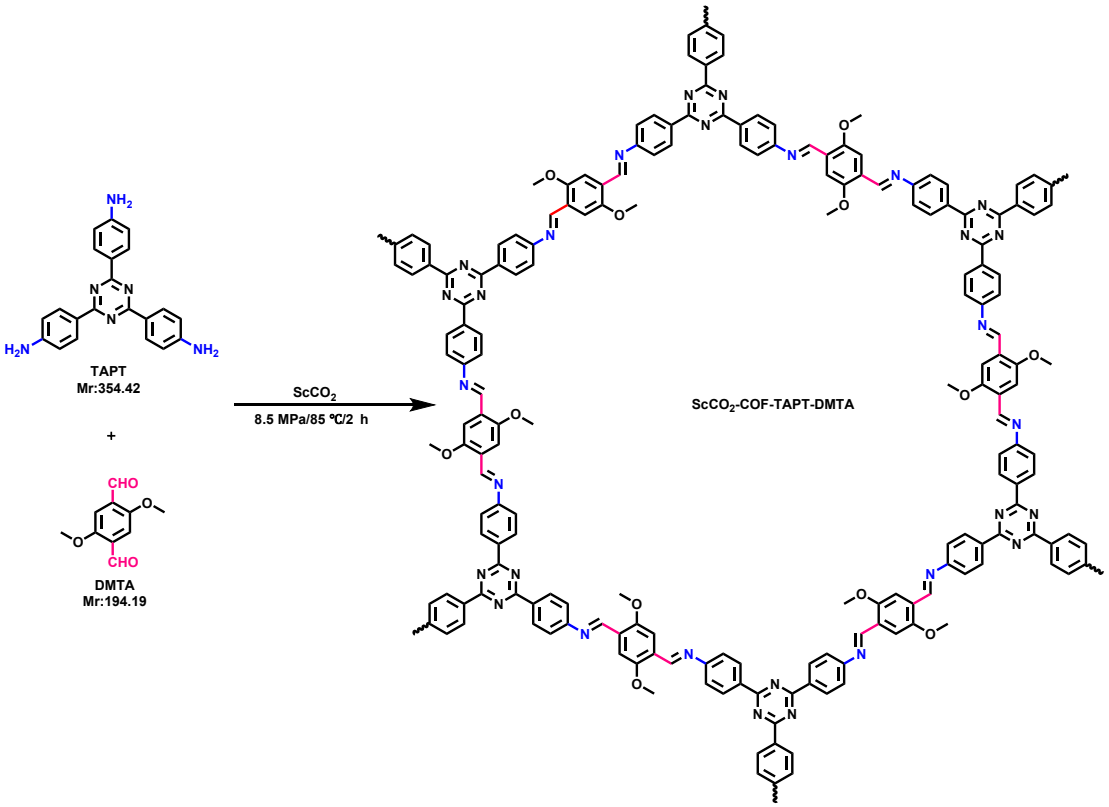

Traditional solvothermal method: The above-mentioned COF was traditionally synthesized in 3 days at 120 °C by using n-butanol (n-BuOH) and o-dichlorobenzene (o-DCB). The reported yield of the COF was 85.3% [3].

The $scCO_2$ method: The $scCO_2$-COF-TAPT-DMTA was obtained in $scCO_2$ according to the general method in 2 hours. The yield of the $scCO_2$-COF-TAPT-DMTA is 56.5%.

Synthesis of $scCO_2$-COF-TAPT-TFB

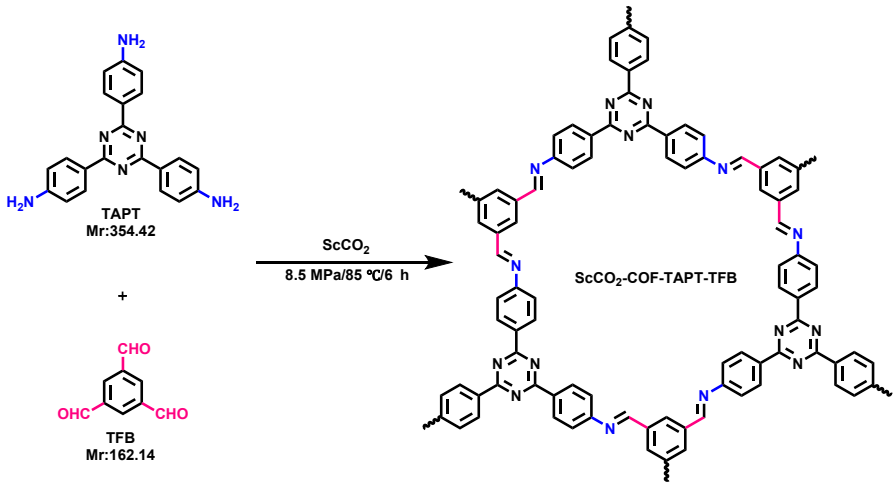

Traditional solvothermal method: The above-mentioned COF was synthesized previously traditionally in 3 days at 120°C by using 1,4-dioxane/mesitylene. The reported yield of the COF was 90 % [4].

The $scCO_2$ Method: The $scCO_2$-COF-TAPT-TFB was obtained according to the general method in 2 hours. The yield of $scCO_2$-COF-TAPT-TFB is 81.7 %.

Synthesis of $scCO_2$-COF-DMTHA-TFB

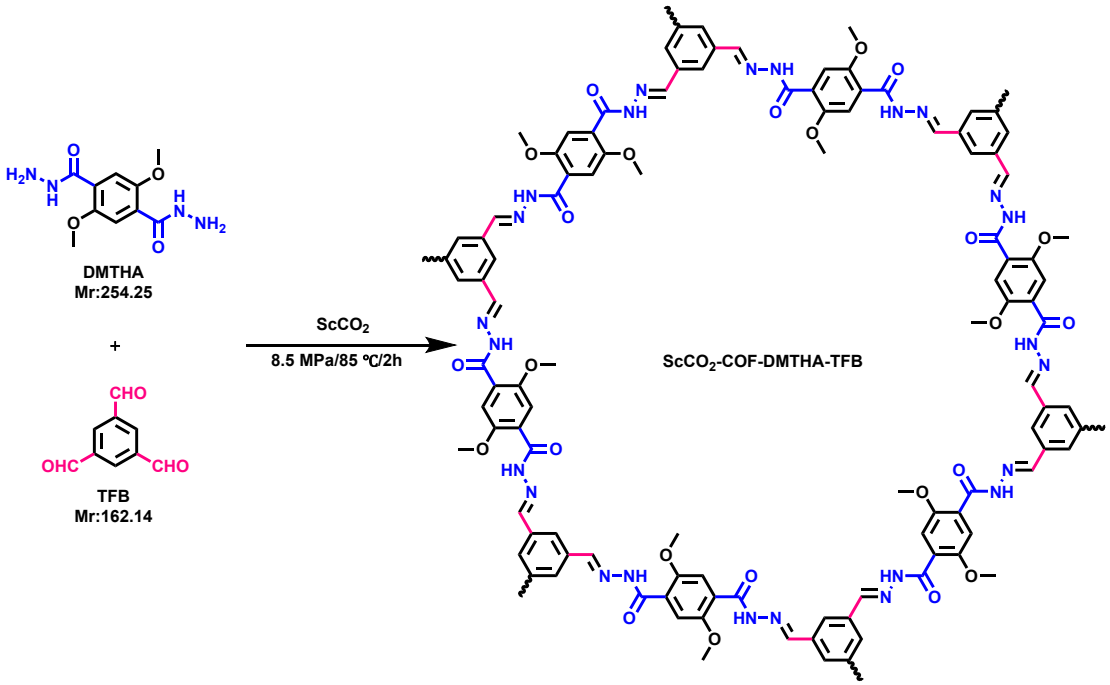

Traditional solvothermal method: The above-mentioned COF was traditionally synthesized in 3 days at 120 °C by using 1,4-dioxane/mesitylene. The reported yield of the COF was 88% [5].

The $scCO_2$ Method: The $scCO_2$-COF-DMTHA-TFB was obtained according to the general method in 2 hours. The yield of $scCO_2$-COF-DMTHA-TFB is 63.7%.

Synthesis of $scCO_2$-COF-BATH-TFB

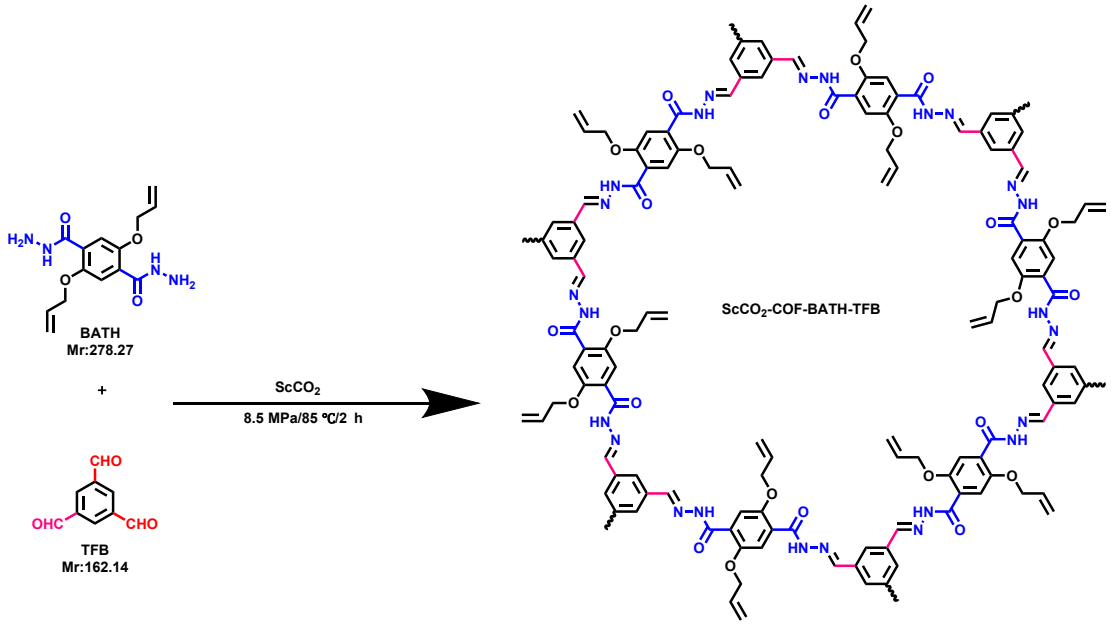

Traditional solvothermal method: The above-mentioned COF was traditionally synthesized in 3 days at 120 °C by using *o*-DCB. The reported yield of the COF was 96% [6].

The $scCO_2$ Method: The $scCO_2$-COF-BATH-TFB was obtained according to the general method in 2 hours. The yield of $scCO_2$-COF-BATH-TFB is 86.5%.

Synthesis of $scCO_2$-COF-TATTA-HH

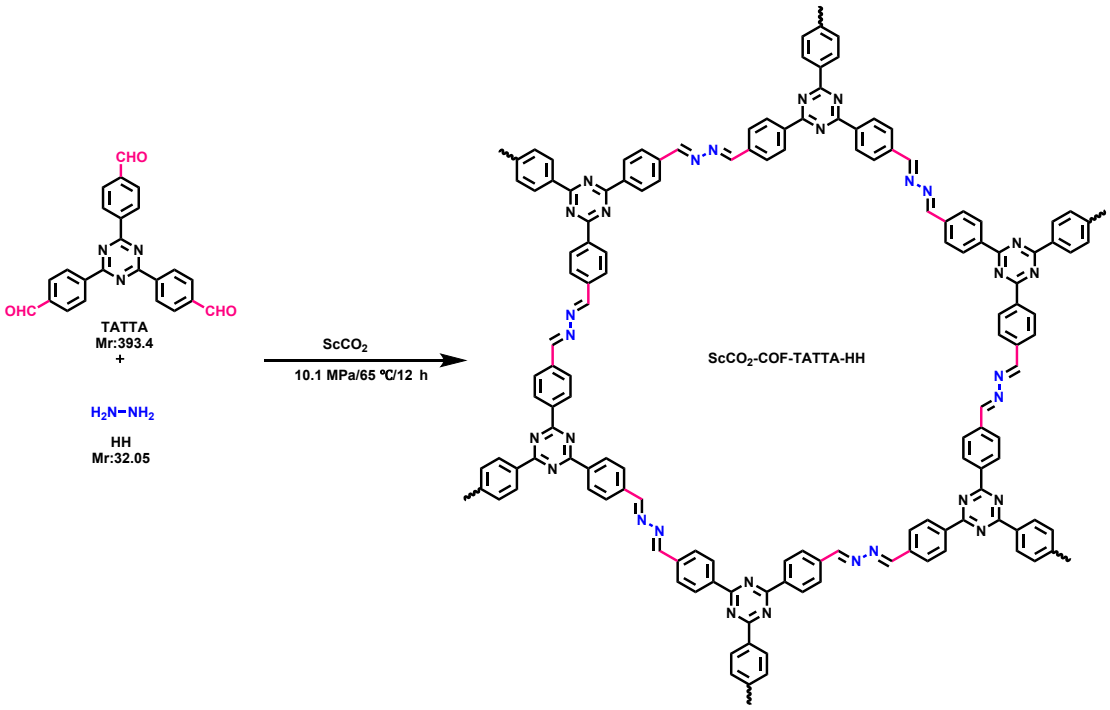

Traditional solvothermal method: The above-mentioned COF was traditionally synthesized in 3 days at 120 °C by using dioxane/1,3,5-trimethylbenzene. The reported yield of the COF was 81% [7].

The $scCO_2$ Method: The $scCO_2$-COF-TATTA-HH was obtained according to the general method in 2 hours. The yield of $scCO_2$-COF-TATTA-HH is 61.2%.

Synthesis of $scCO_2$-COF-TFPB-HH

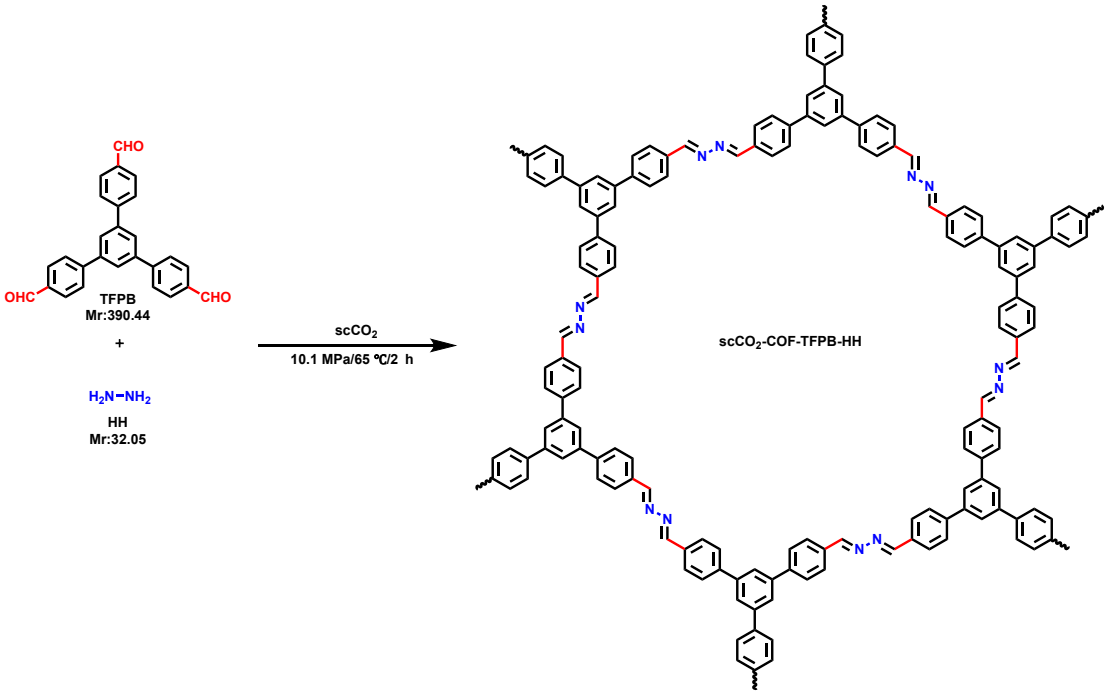

Traditional solvothermal method: The above-mentioned COF was traditionally synthesized in 3 days at 120 °C by using benzoic anhydride (BZDA). The reported yield of the COF was 73% [8].

The $scCO_2$ Method: The $scCO_2$-COF-TFPB-HH was obtained according to the general method in 2 hours. The yield of $scCO_2$-COF-TFPB-HH is 47.0%.

Synthesis of $scCO_2$-COF-TATTA-TMT

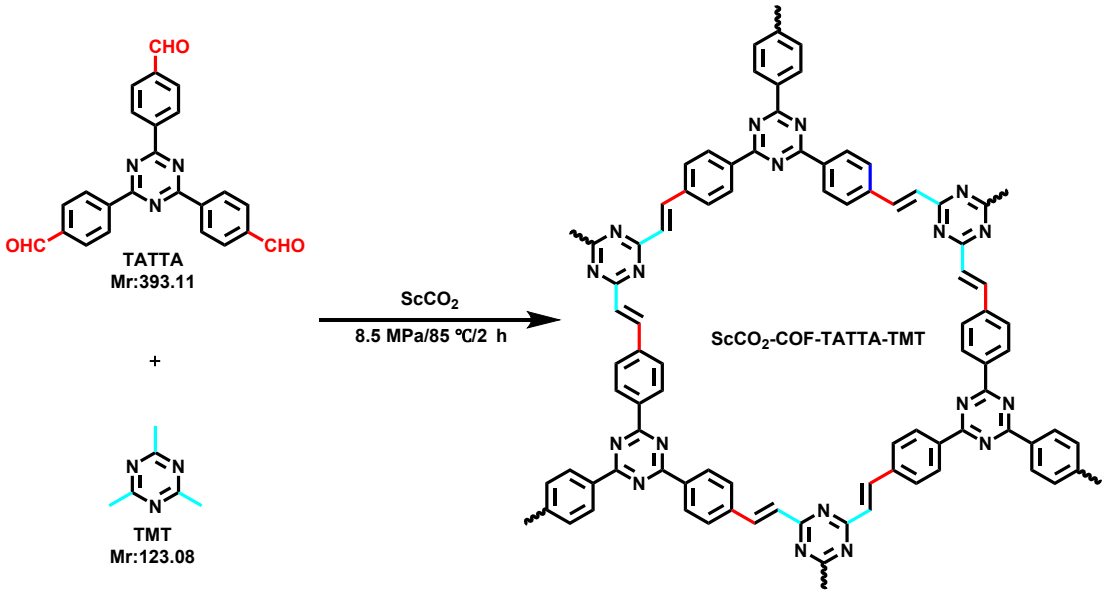

Traditional solvothermal method: The above-mentioned COF was traditionally synthesized in 3 days at 150 °C by using dioxane/1,3,5-trimethylbenzene as solvent and trifluoroacetic acid as catalyst [9].

The $scCO_2$ Method: The $scCO_2$-COF-TATTA-TMT was obtained according to the general method in 2 hours. The yield of $scCO_2$-COF-TATTA-TMT is 77.9%.

Characteristics of $scCO_2$-COFs

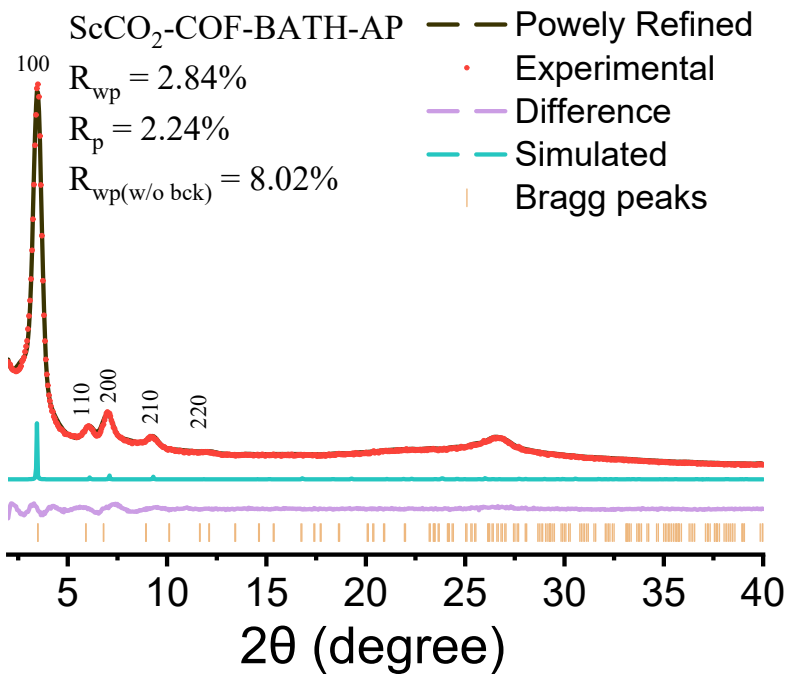

Figure S1a. PXRD pattern of $scCO_2$-COF-BATH-AP.

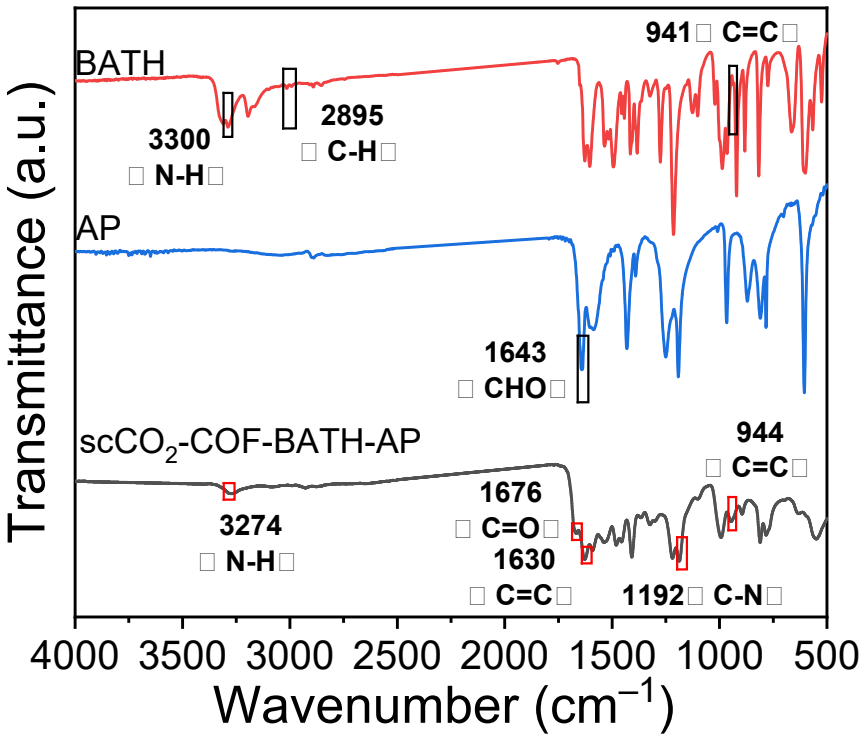

Figure S1b. FT-IR spectra of $scCO_2$-COF-BATH-AP, and starting materials, BATH and AP.

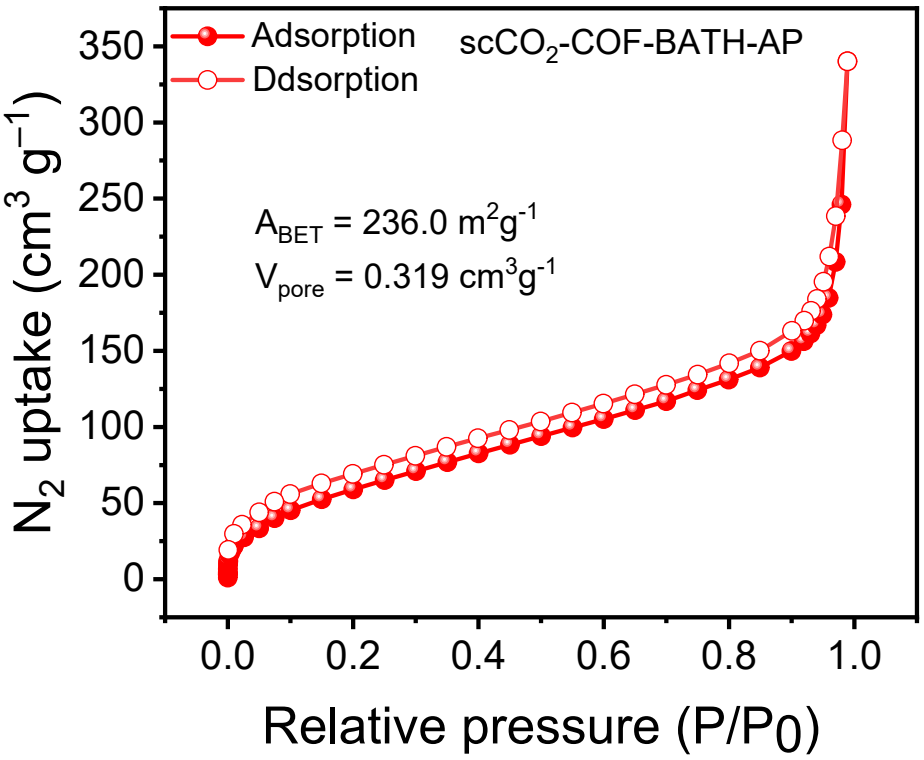

Figure S1c. N_2 adsorption and desorption profiles of $scCO_2$-COF-BATH-AP.

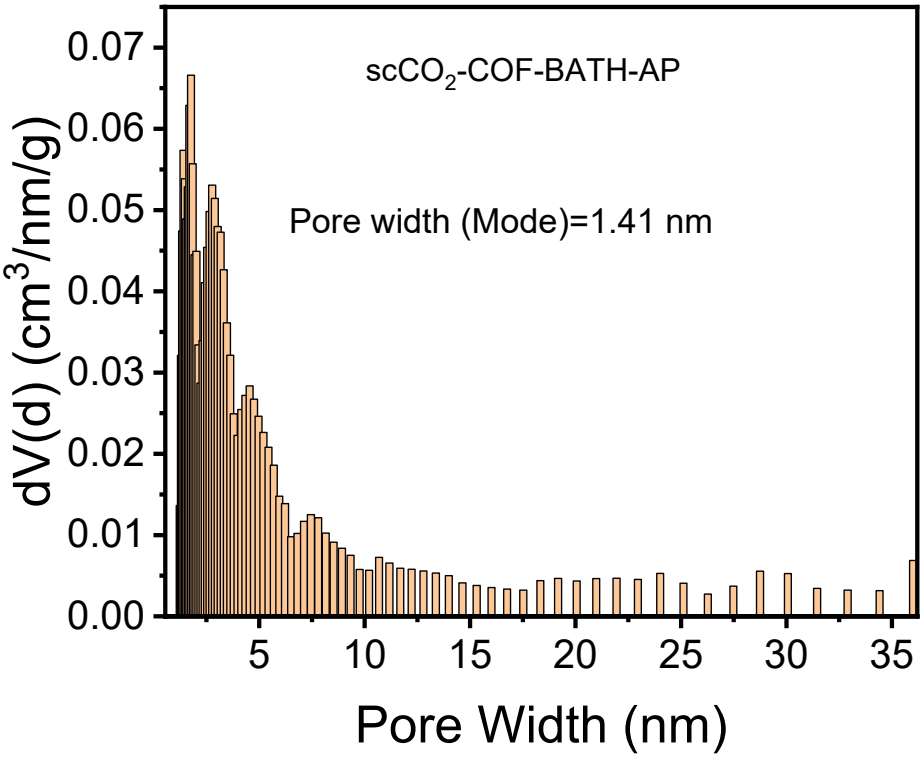

Figure S1d. Pore size distribution profile of $scCO_2$-COF-BATH-AP.

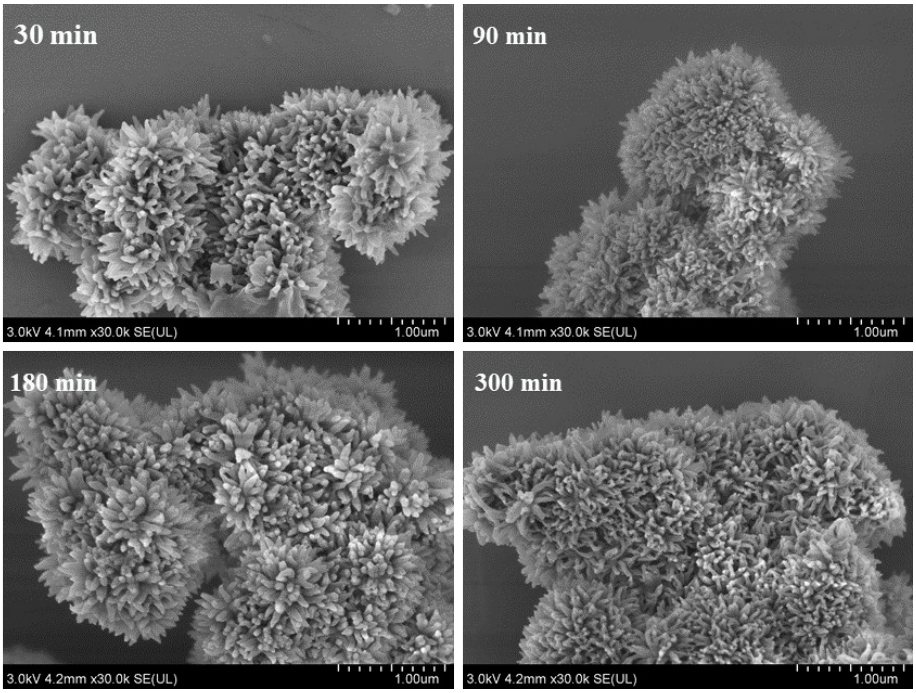

Figure S2. SEM images of $scCO_2$-COF-BATH-AP samples synthesized at different reaction times.

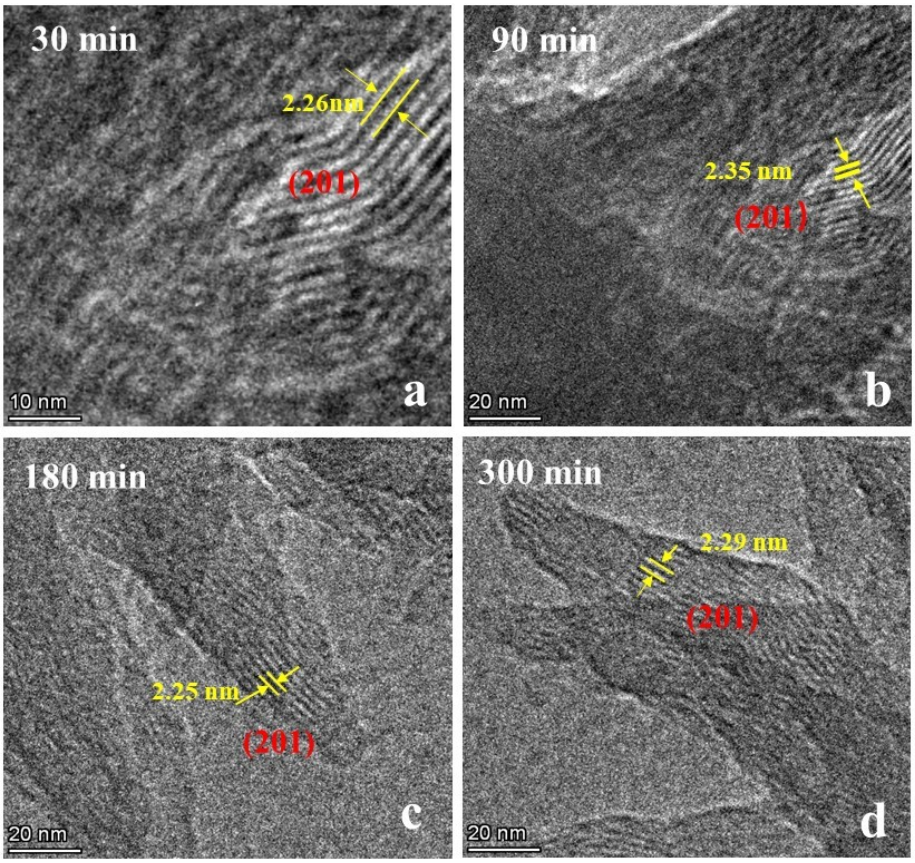

Figure S3. TEM images of $scCO_2$-COF-BATH-AP samples synthesized at different reaction times.

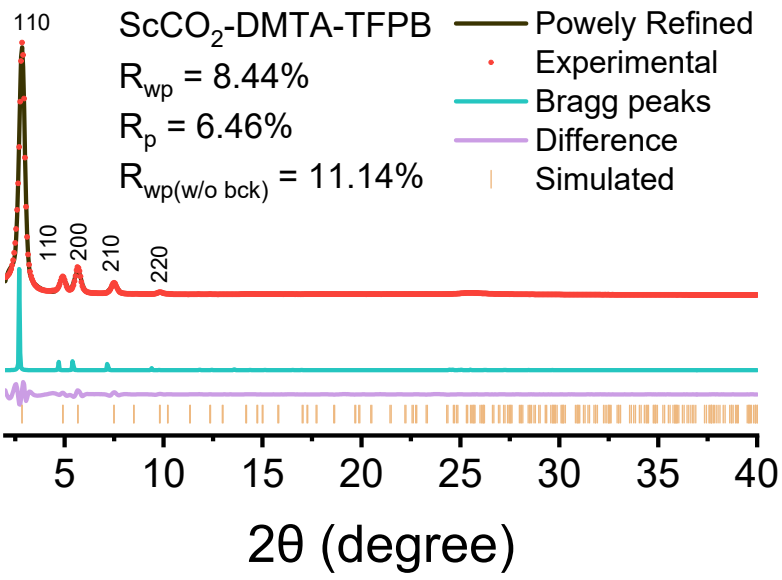

Figure S4a. PXRD pattern of $scCO_2$-COF-TAPB-DMTA.

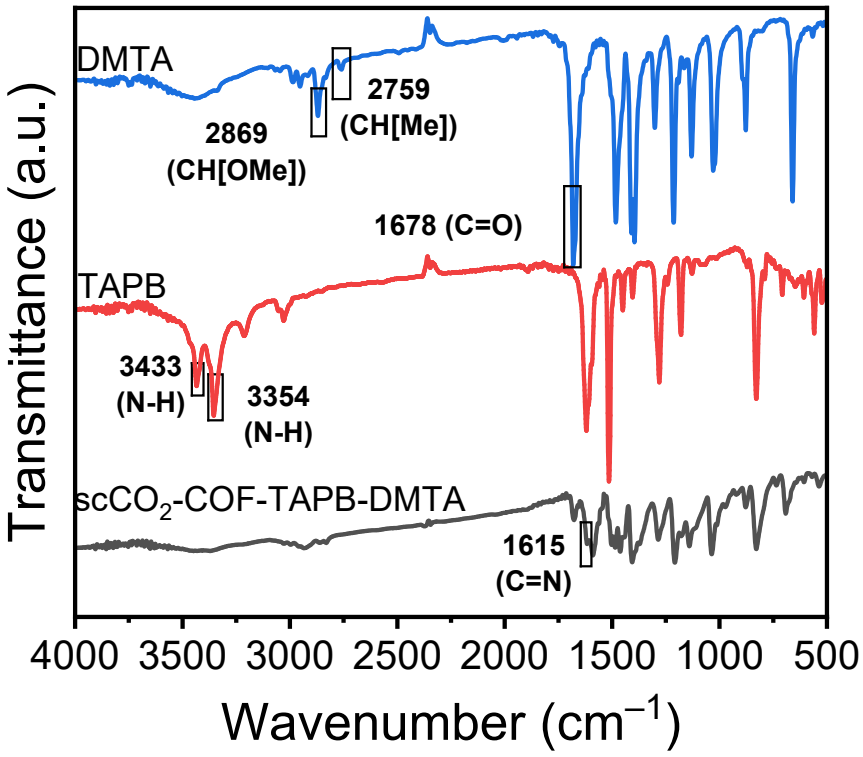

Figure S4b. FT-IR of $scCO_2$-COF-TAPB-DMTA, and starting materials, TAPB and DMTA.

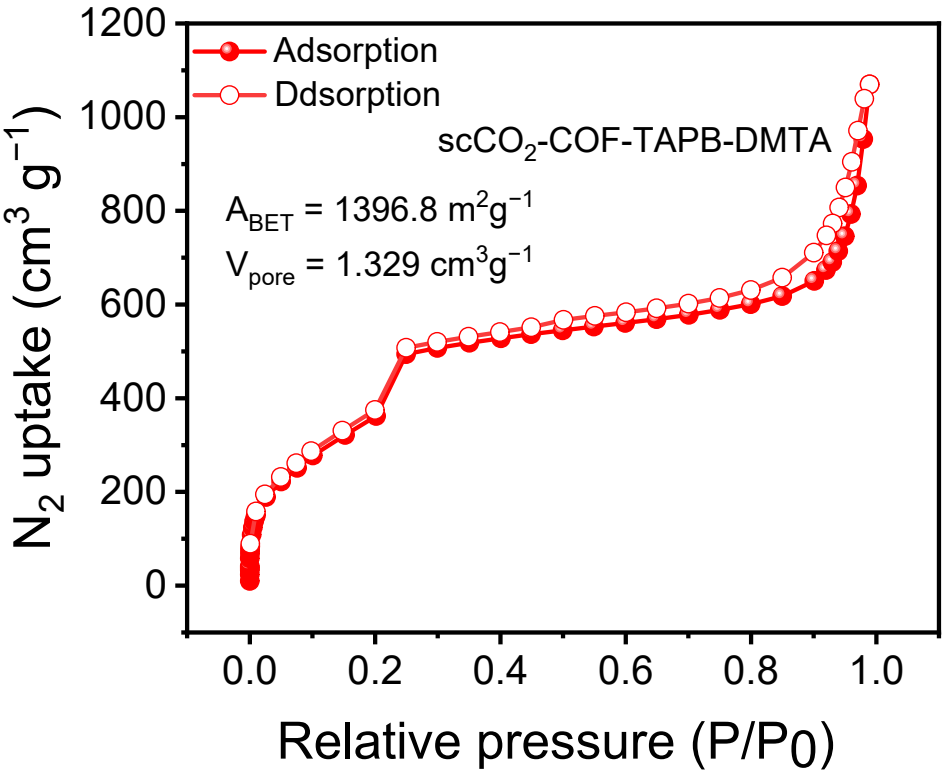

Figure S4c. N_2 adsorption and desorption profiles of $scCO_2$-COF-TAPB-DMTA.

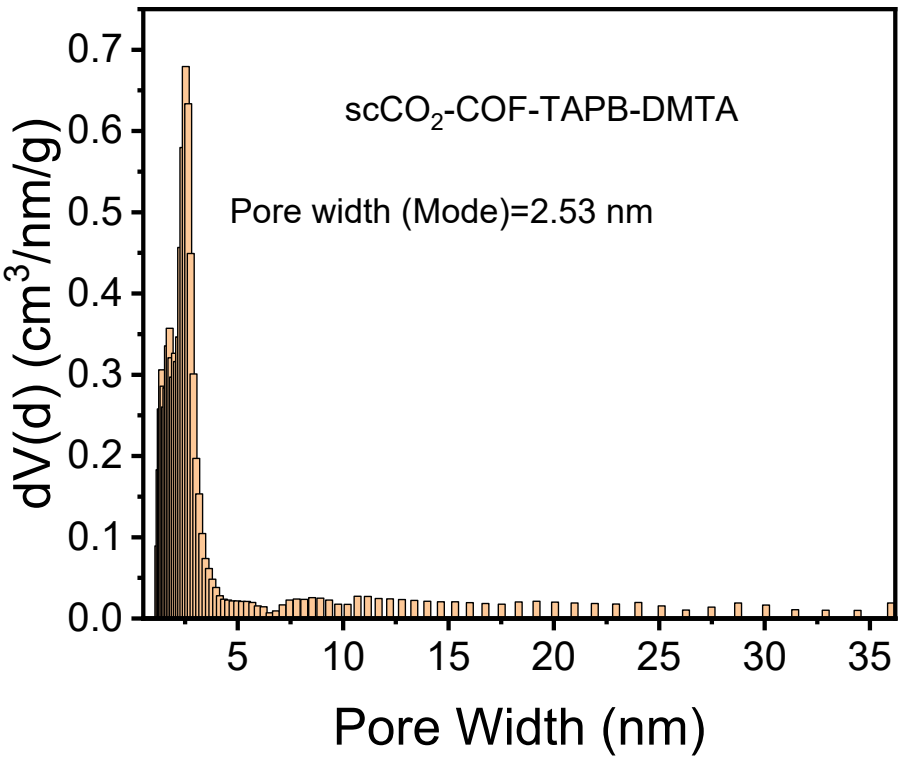

Figure S4d. Pore size distribution profile of $scCO_2$-COF-TAPB-DMTA.

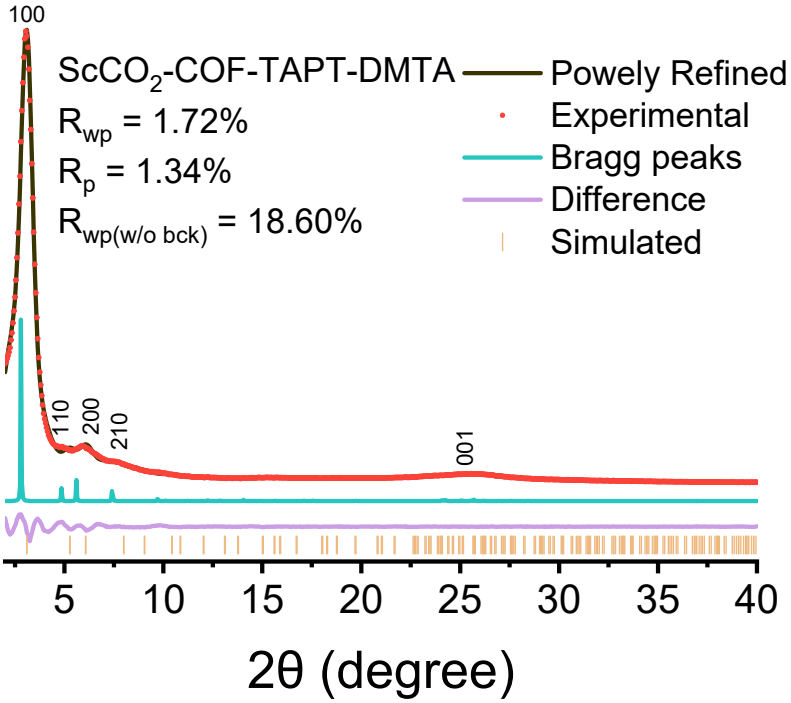

Figure S5a. PXRD pattern of scCO$_2$-COF-TAPT-DMTA.

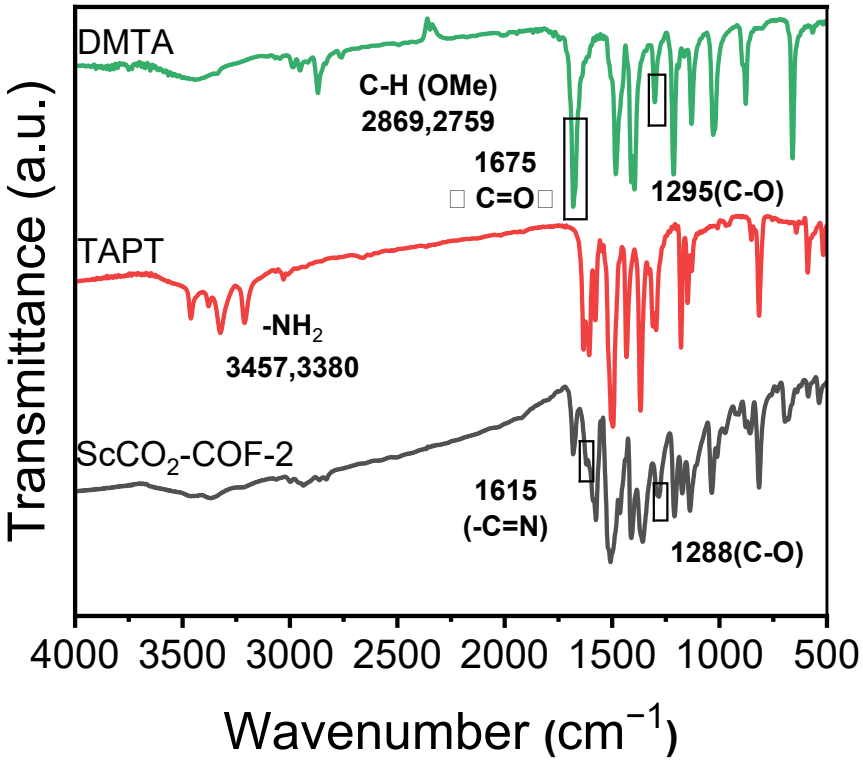

Figure S5b. FT-IR of scCO$_2$-COF-TAPT-DMTA, and starting materials, TAPT and DMTA.

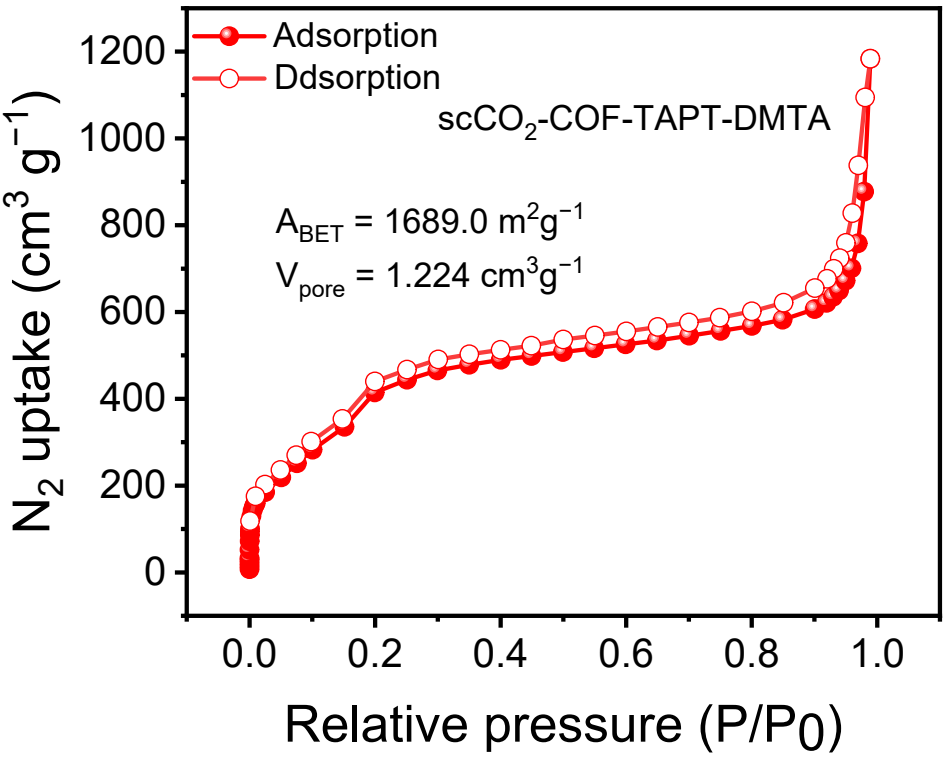

Figure S5c. N_2 adsorption and desorption profiles of $scCO_2$-COF-TAPT-DMTA.

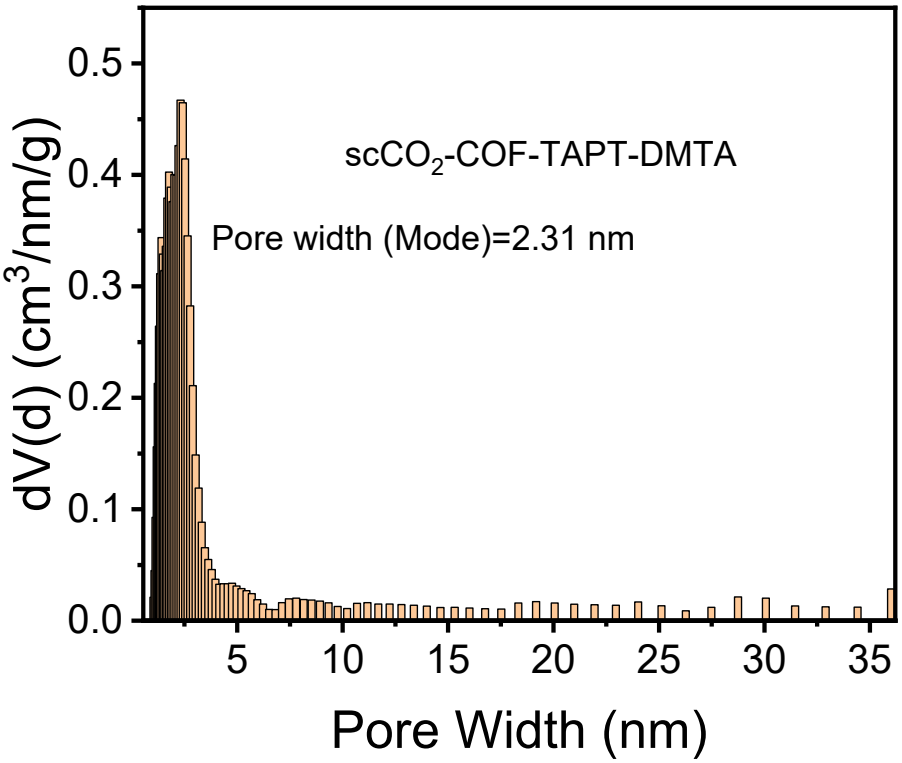

Figure S5d. Pore size distribution profile of $scCO_2$-COF-TAPT-DMTA.

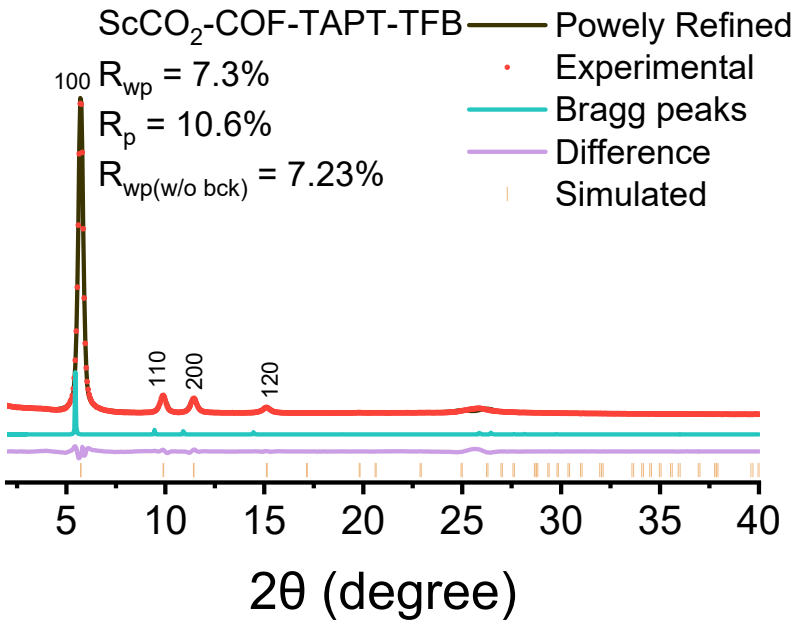

Figure S6a. PXRD pattern of $scCO_2$-COF-TAPT-TFB.

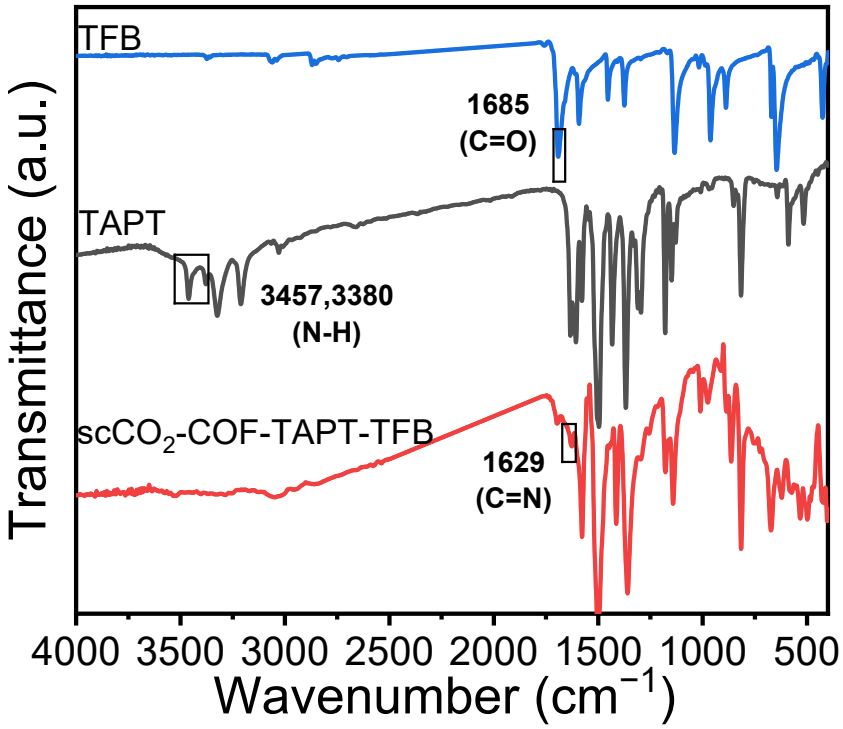

Figure S6b. FT-IR of $scCO_2$-COF-TAPT-TFB, and starting materials, TAPT and TFB.

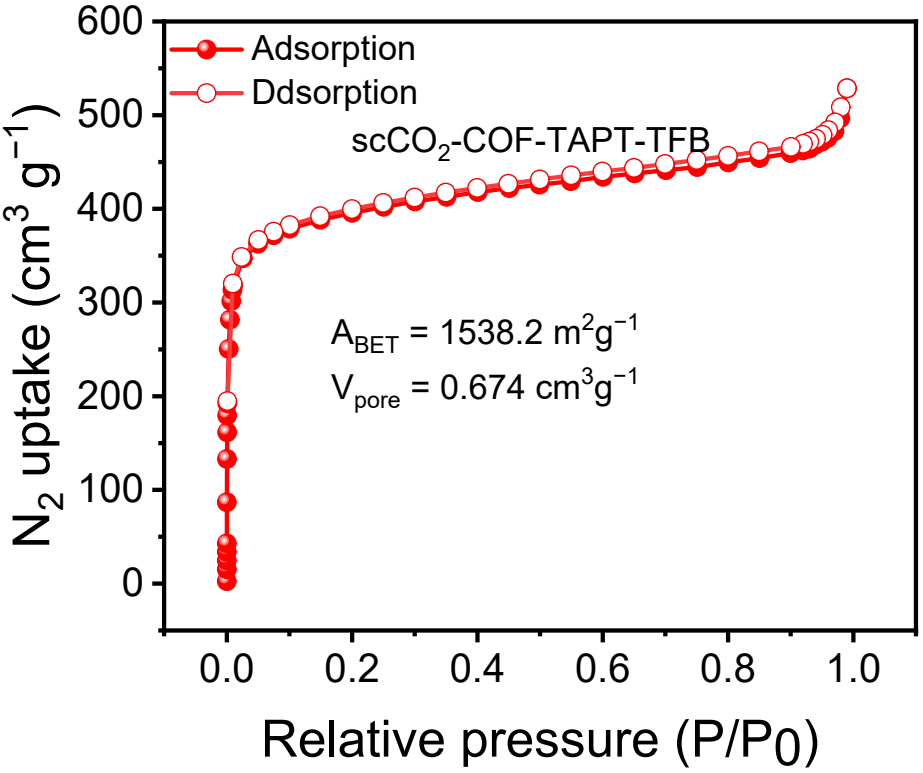

Figure S6c. N_2 adsorption and desorption profiles of $scCO_2$-COF-TAPT-TFB.

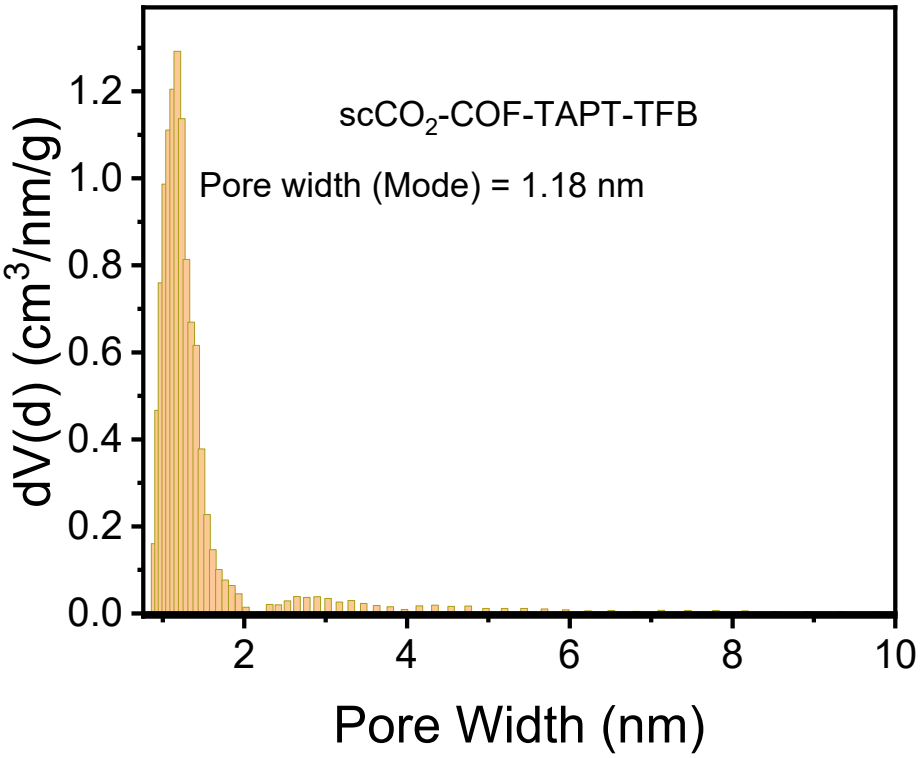

Figure S6d. Pore size distribution profile of $scCO_2$-COF-TAPT-TFB.

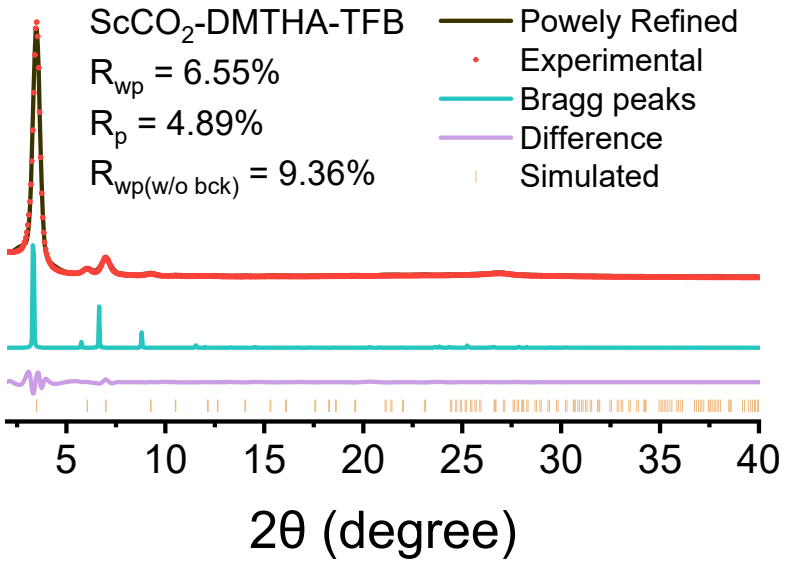

Figure S7a. PXRD pattern of $scCO_2$-COF-DMTHA-TFB.

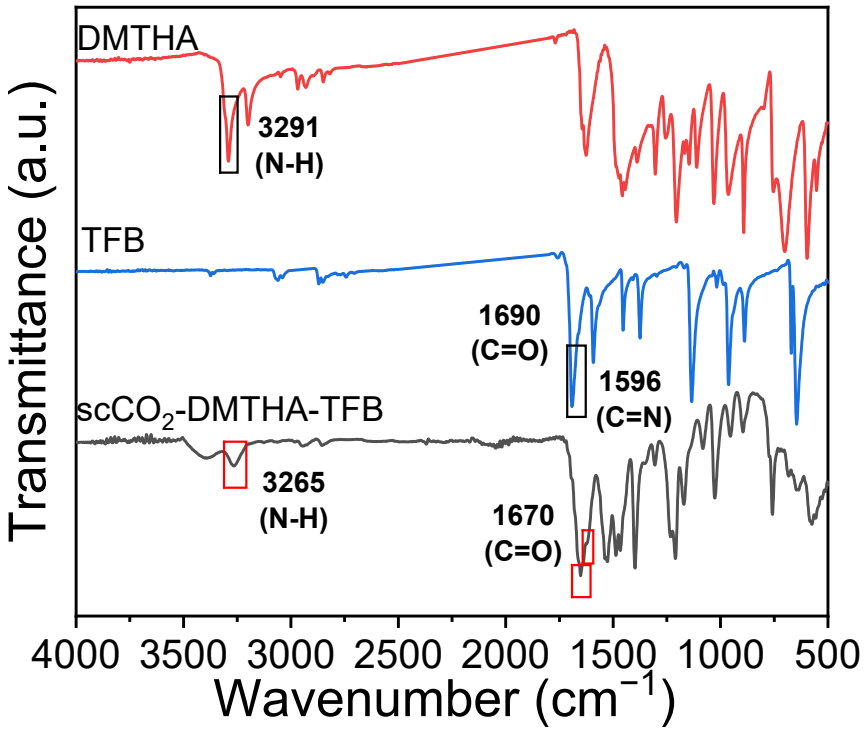

Figure S7b. FT-IR of $scCO_2$-COF-DMTHA-TFB, and starting materials, DMTHA and TFB.

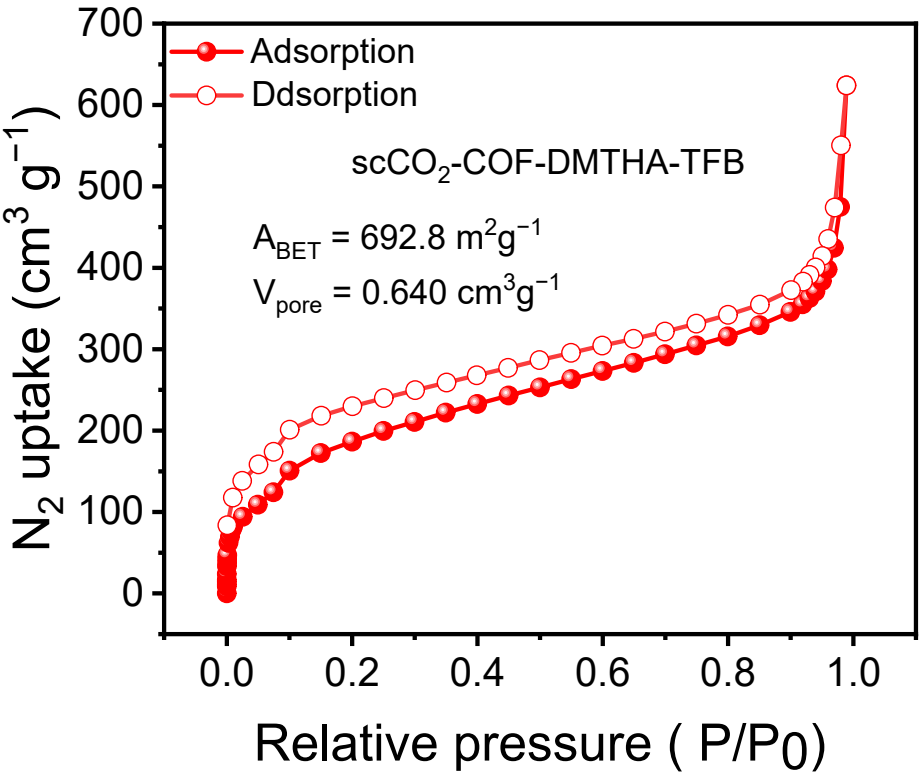

Figure S7c. N_2 adsorption and desorption profiles of $scCO_2$-COF-DMTHA-TFB.

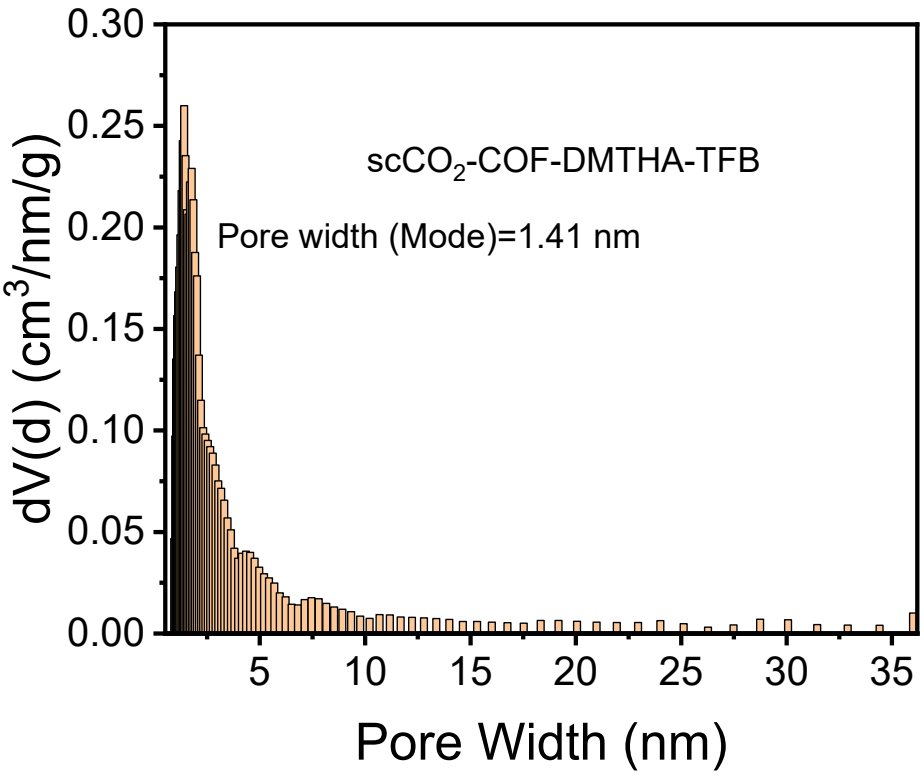

Figure S7d. Pore size distribution profile of $scCO_2$-COF-DMTHA-TFB.

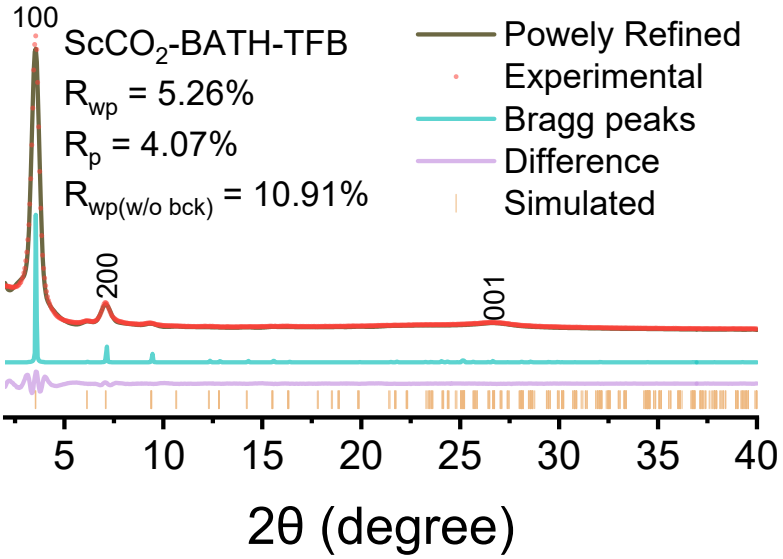

Figure S8a. PXRD pattern of $scCO_2$-COF-BATH-TFB.

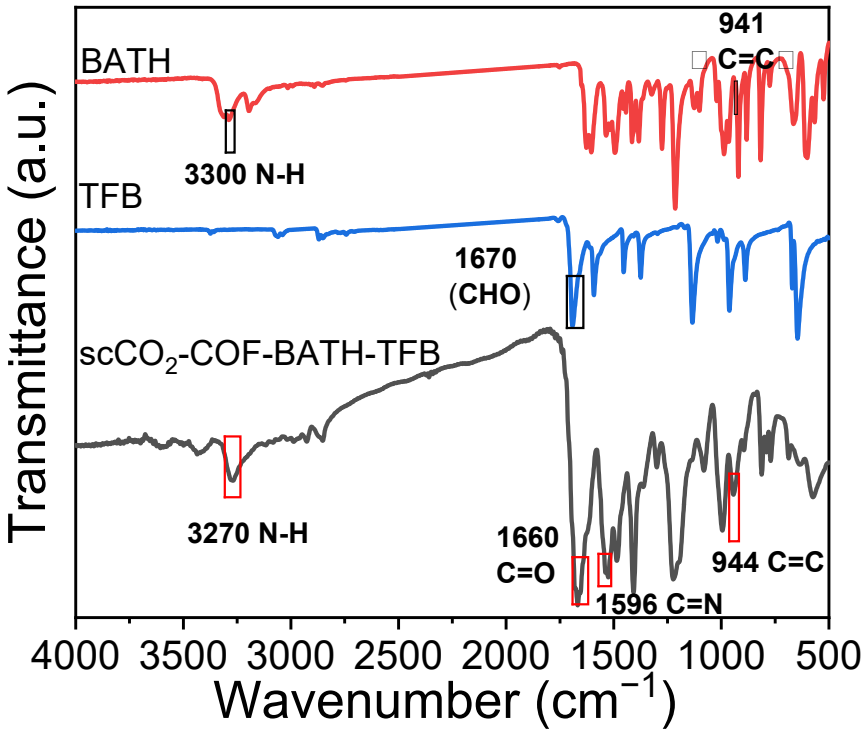

Figure S8b. FT-IR of $scCO_2$-COF-BATH-TFB, and starting materials, BATH and TFB.

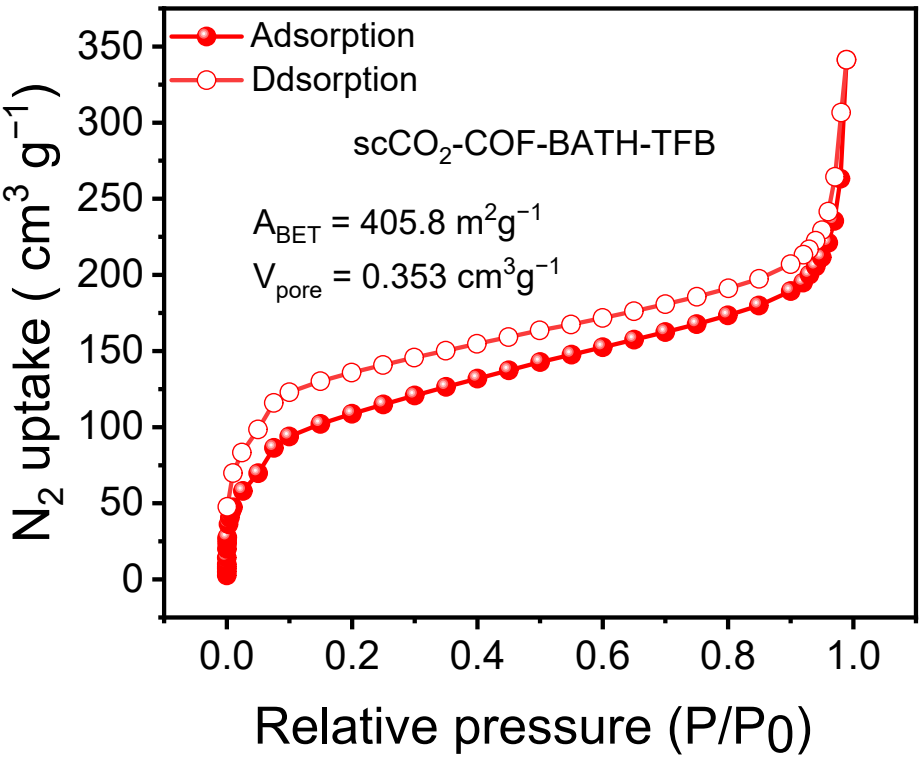

Figure S8c. N_2 adsorption and desorption profiles of $scCO_2$-COF-BATH-TFB.

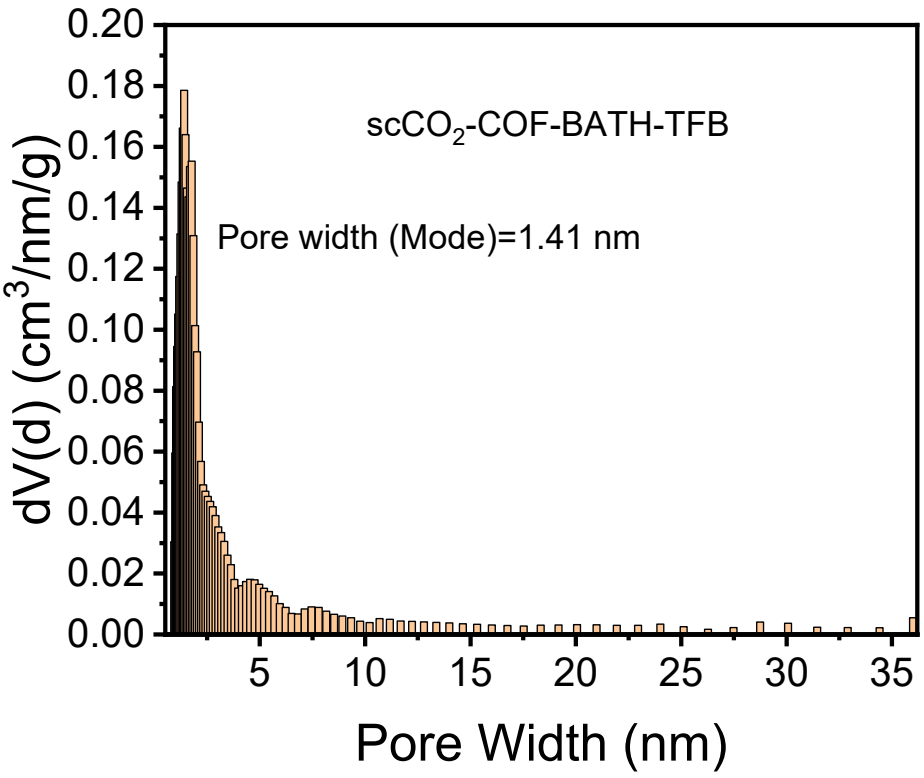

Figure S8d. Pore size distribution profile of $scCO_2$-COF-BATH-TFB.

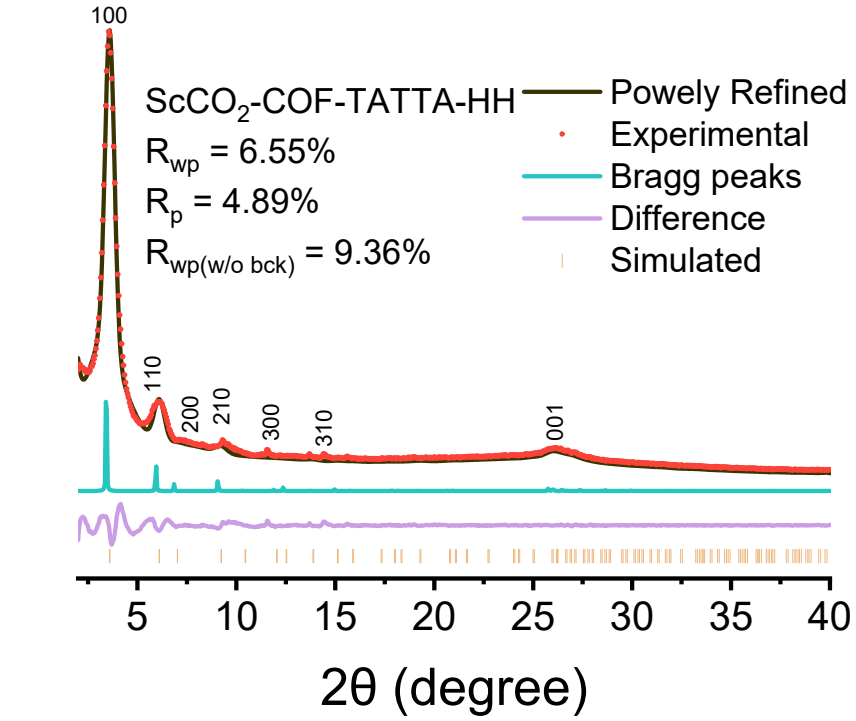

Figure S9a. PXRD pattern of $scCO_2$-COF-TATTA-HH.

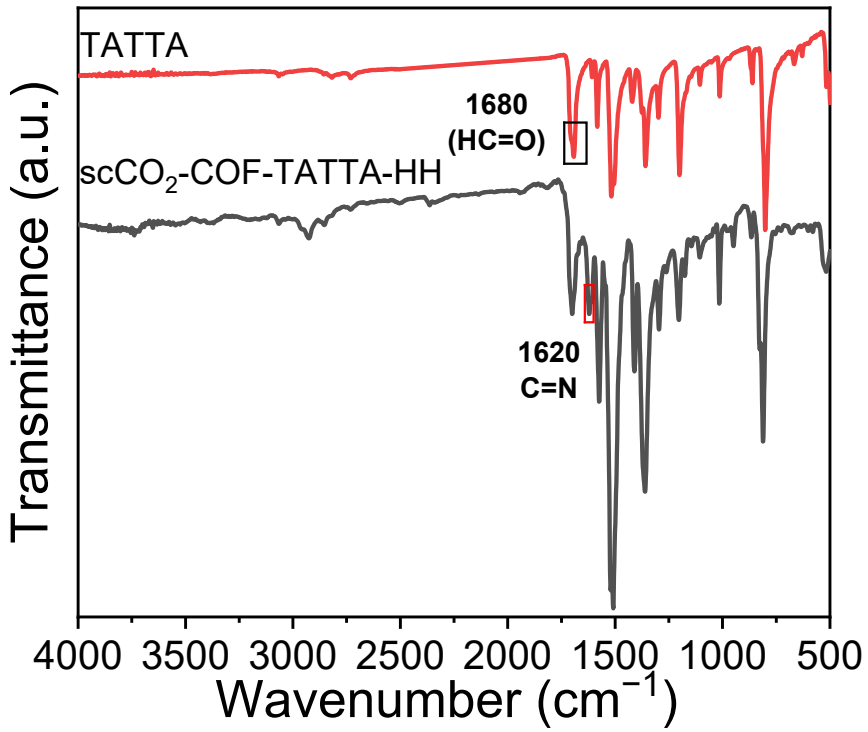

Figure S9b. FT-IR of $scCO_2$-COF-TATTA-HH, and starting materials, TATTA and HH.

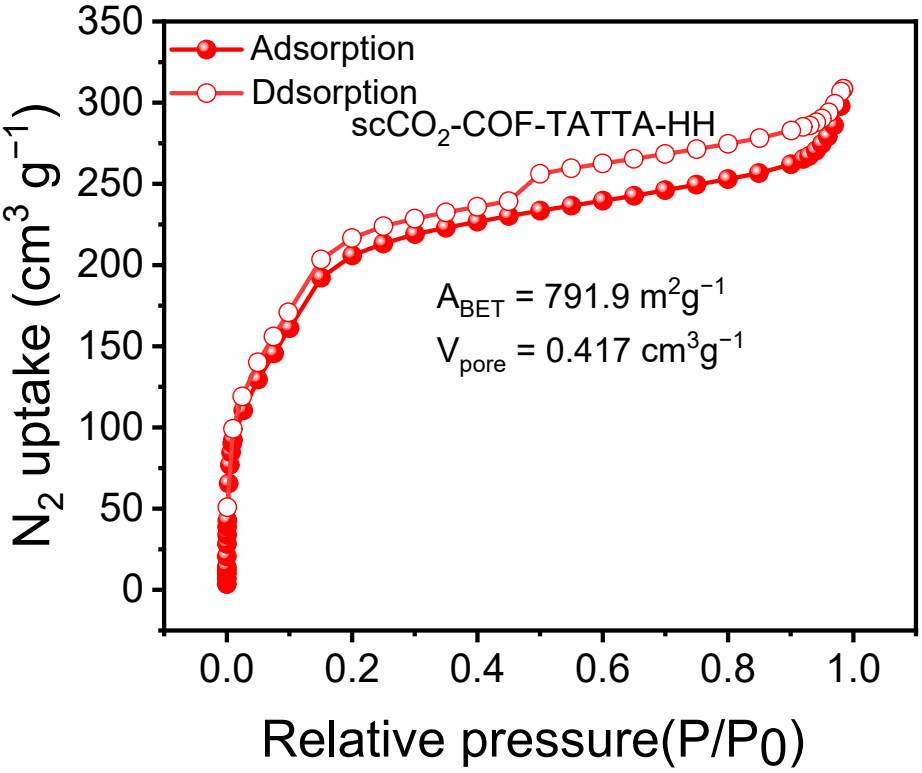

Figure S9c. N_2 adsorption and desorption profiles of $scCO_2$-COF-TATTA-HH.

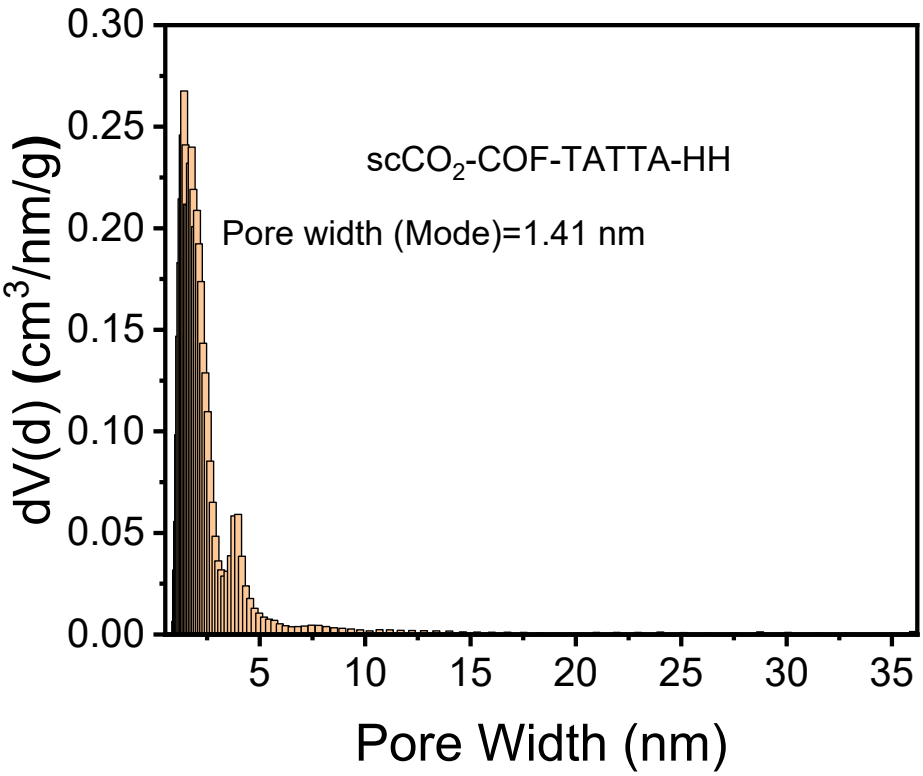

Figure S9d. Pore size distribution profile of $scCO_2$-COF-TATTA-HH.

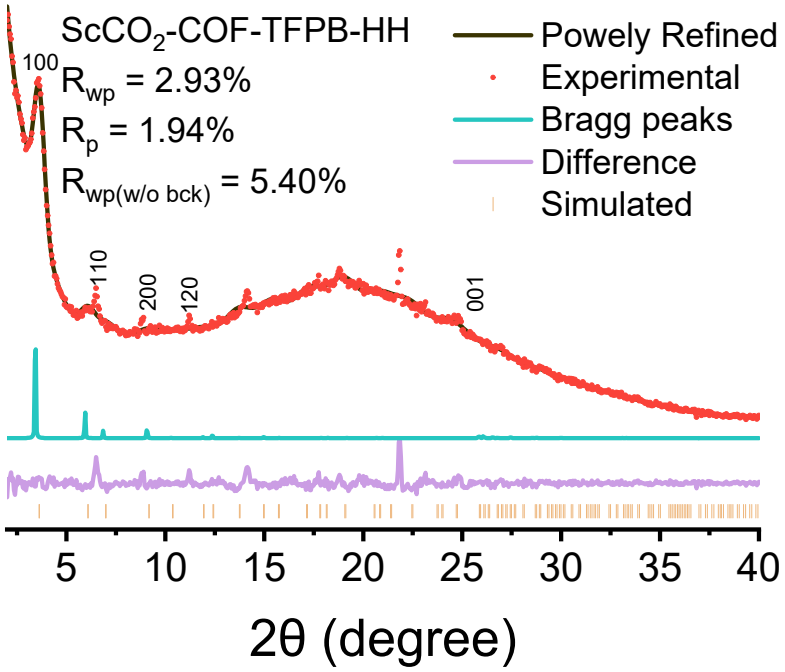

Figure S10a. PXRD pattern of $scCO_2$-COF-TFPB-HH.

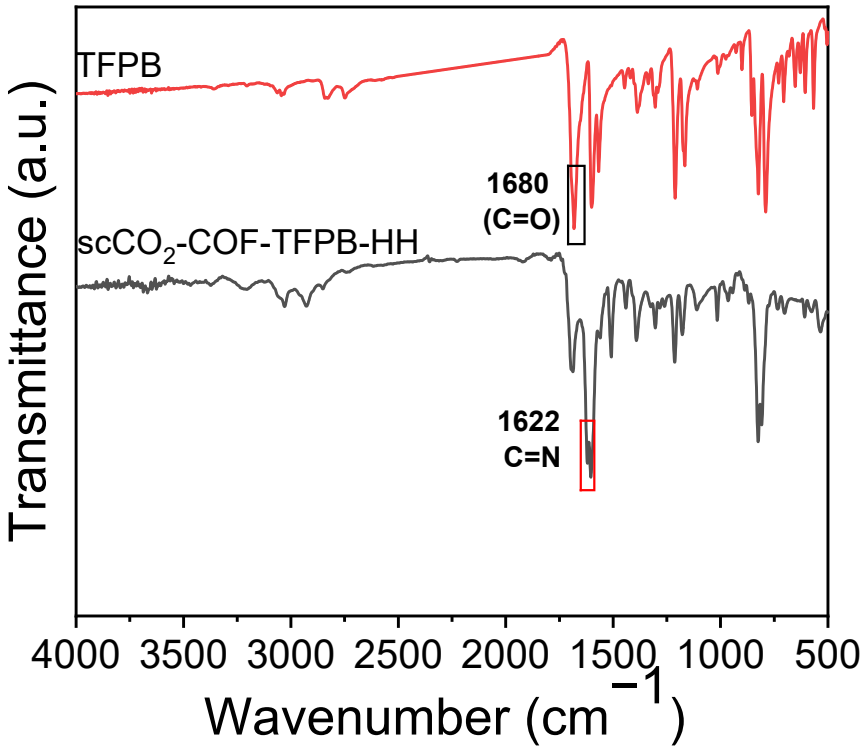

Figure S10b. FT-IR of $scCO_2$-COF-TFPB-HH, and starting materials, TFPB and HH.

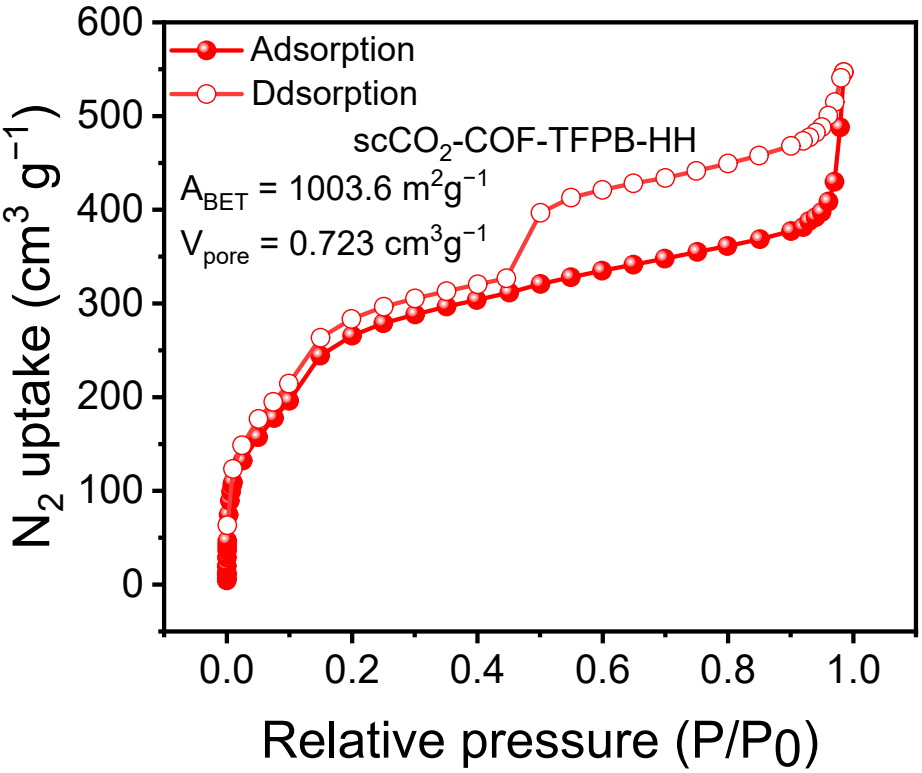

Figure S10c. N_2 adsorption and desorption profiles of $scCO_2$-COF-TFPB-HH.

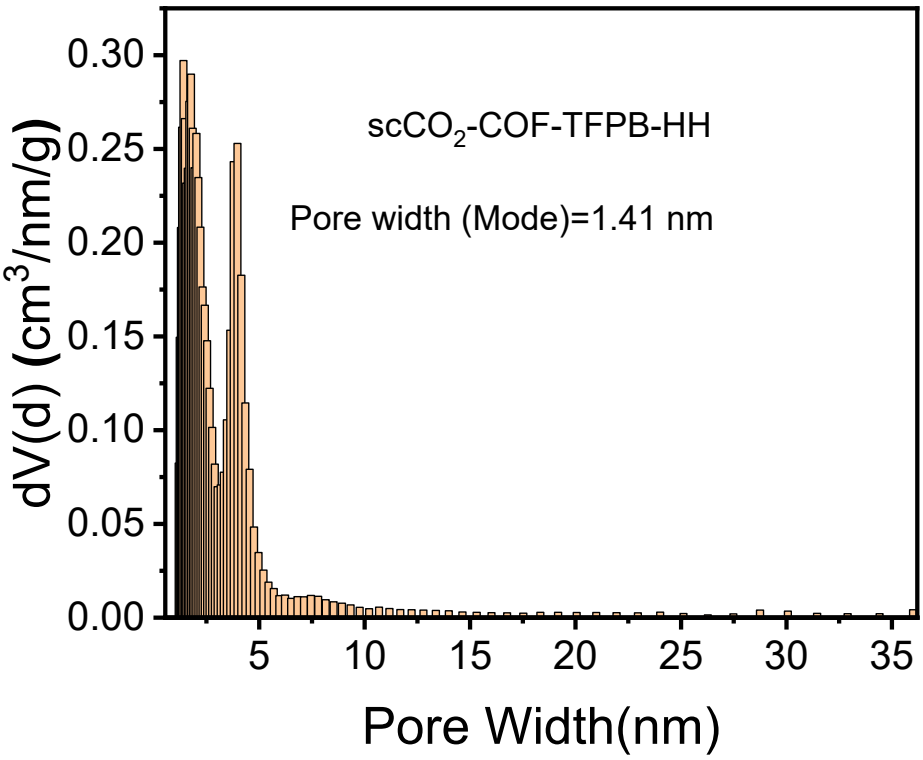

Figure S10d. Pore size distribution profile of $scCO_2$-COF-TFPB-HH.

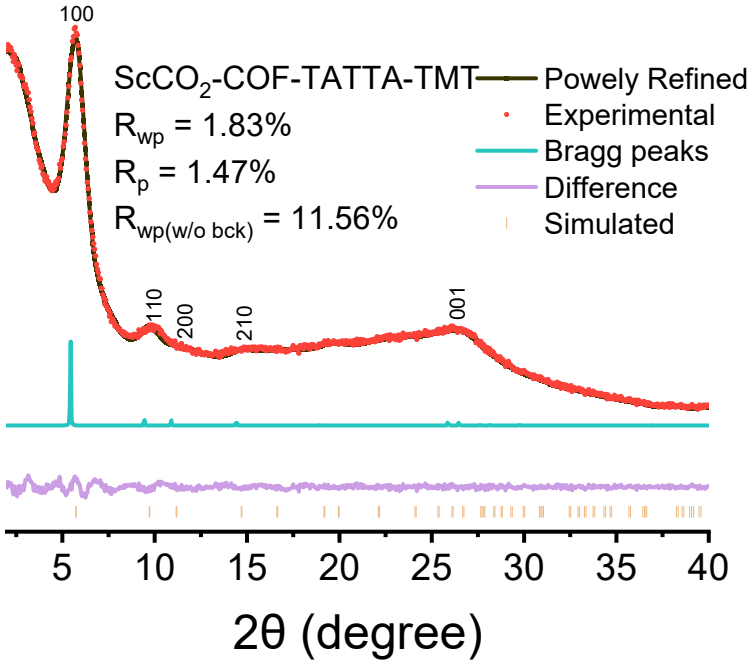

Figure S11a. PXRD pattern of $scCO_2$-COF-TATTA-TMT.

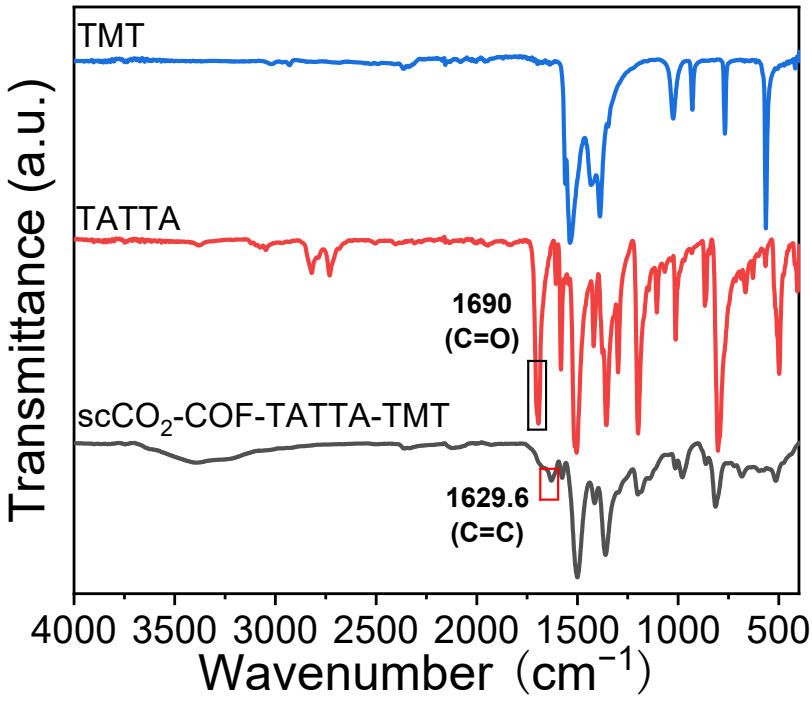

Figure S11b. FT-IR of $scCO_2$-COF-TATTA-TMT, and starting materials, TATTA and TMT.

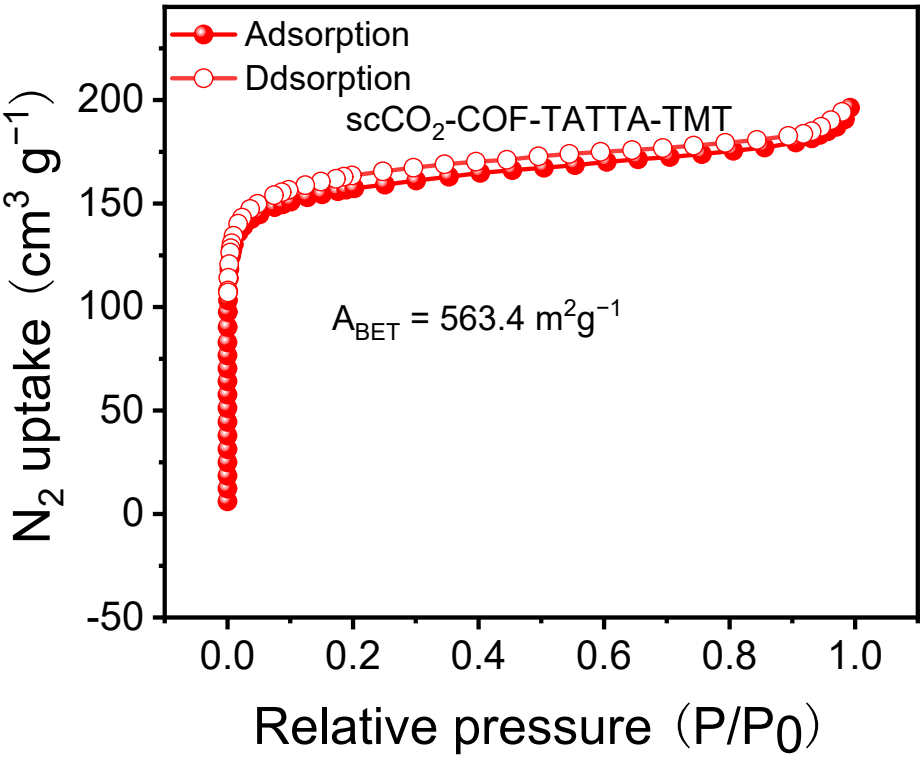

Figure S11c. N_2 adsorption and desorption profiles of $scCO_2$-COF-TATTA-TMT.

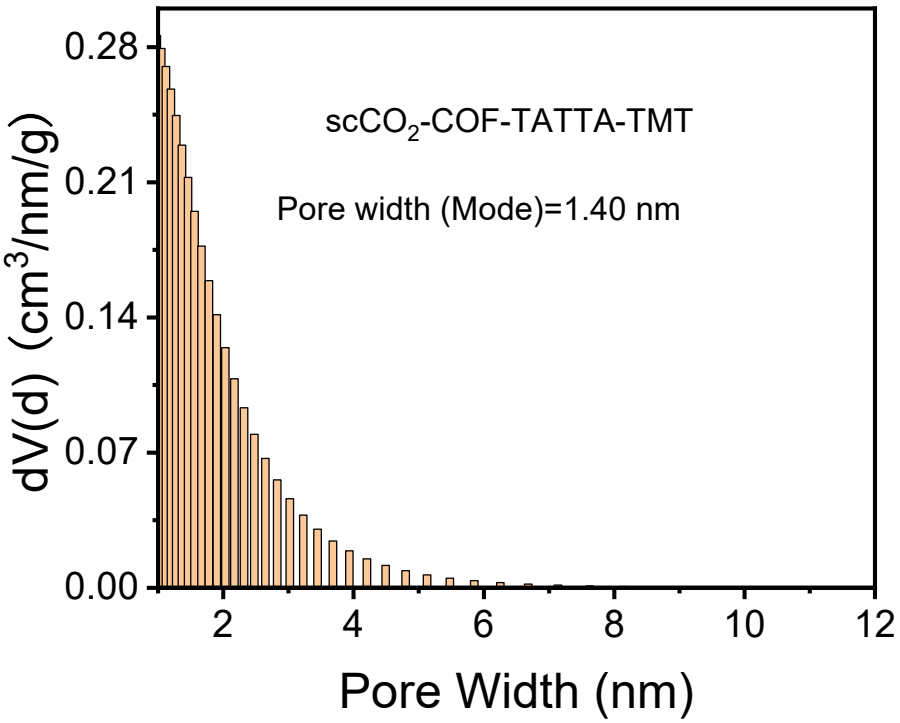

Figure S11d. Pore size distribution profile of $scCO_2$-COF-TATTA-TMT.

Iodine vapor adsorption experimental procedure

Place 10 mg of $scCO_2$-COFs and an excess amount of iodine into two 5 mL airtight bottles. Then, place these bottles into two larger 50 mL airtight bottles. Transfer the larger airtight bottles to a 348 K oven to conduct the iodine vapor adsorption experiment under ambient pressure. The weight of the vials containing the $scCO_2$-COFs was measured at different exposure times, allowing the adsorption curves of the samples to be plotted. The iodine vapor adsorption capacity of $scCO_2$-COFs is calculated using the following equation.

The iodine adsorption capacity is determined using the following formula:

$$\alpha = \frac{(m_2 - m_1)}{m_1}$$

Here, α denotes the iodine vapor adsorption capacity, while m_1 and m_2 represent the weight of the $scCO_2$-COFs sample before and after iodine adsorption, respectively.

Desorption Experiments and reusability measurement

A sample of iodine-loaded $scCO_2$-COFs (0.1 mg) was placed in a colorimetric dish, followed by the addition of 3 mL of methanol solution to immerse the iodine-loaded $scCO_2$-COFs. The methanol solution was then analyzed using a UV-VIS spectrophotometer at three-minute intervals. By testing methanol solutions with varying iodine concentrations, a standard curve was generated to calculate the iodine release from the $scCO_2$-COFs.

The recyclability experiment was carried out by refluxing iodine-loaded $scCO_2$-COFs in methanol solution for 24 hours by Soxhlet extraction, drying the sample at 80 °C for 48 hours, and then performing iodine vapor adsorption experiment again. The same process is repeated for 5 cycles.

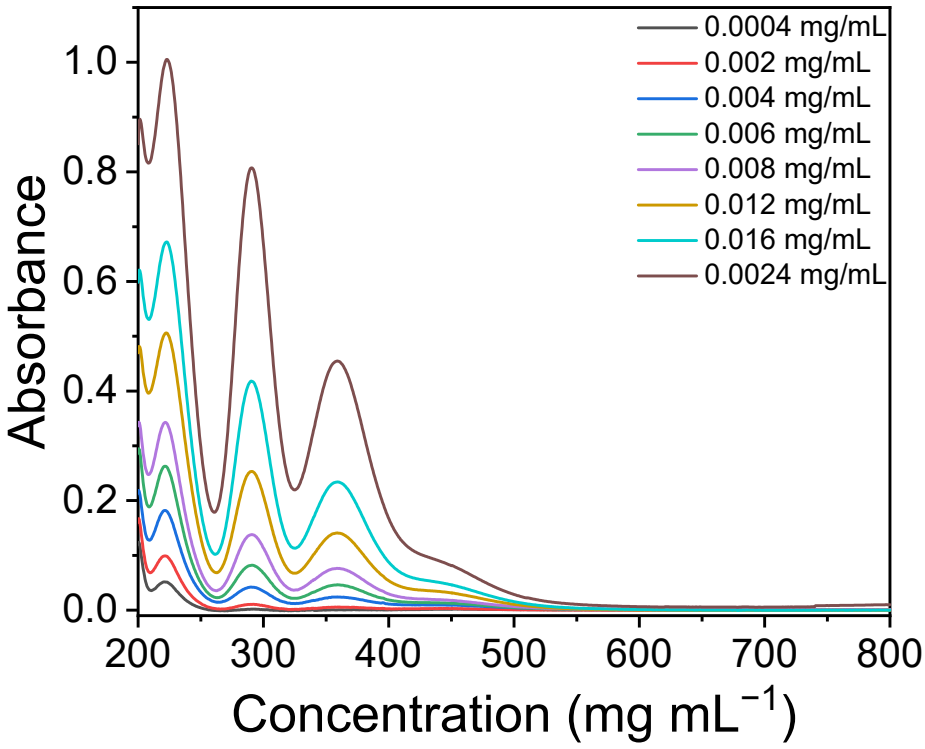

Figure S12a. UV-Vis spectra of methanol standard solutions with different concentrations of iodine.

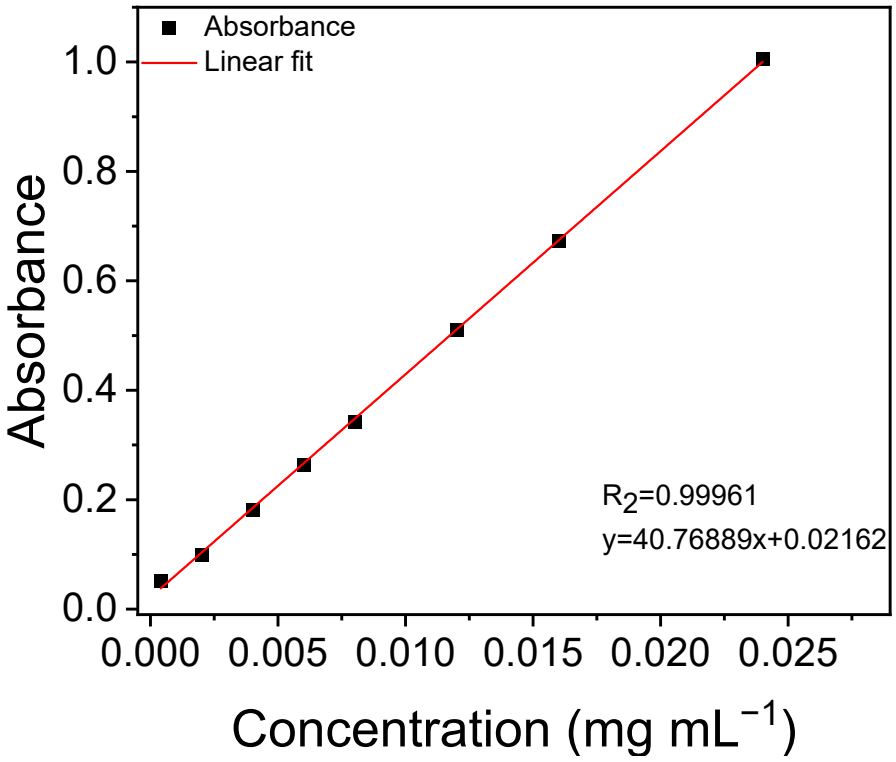

Figure S12b. The corresponding standard curve of absorbance and iodine concentration based on the UV-Vis spectra shown in Figure S9a.

Iodine release behavior of $scCO_2$-COFs in methanol:

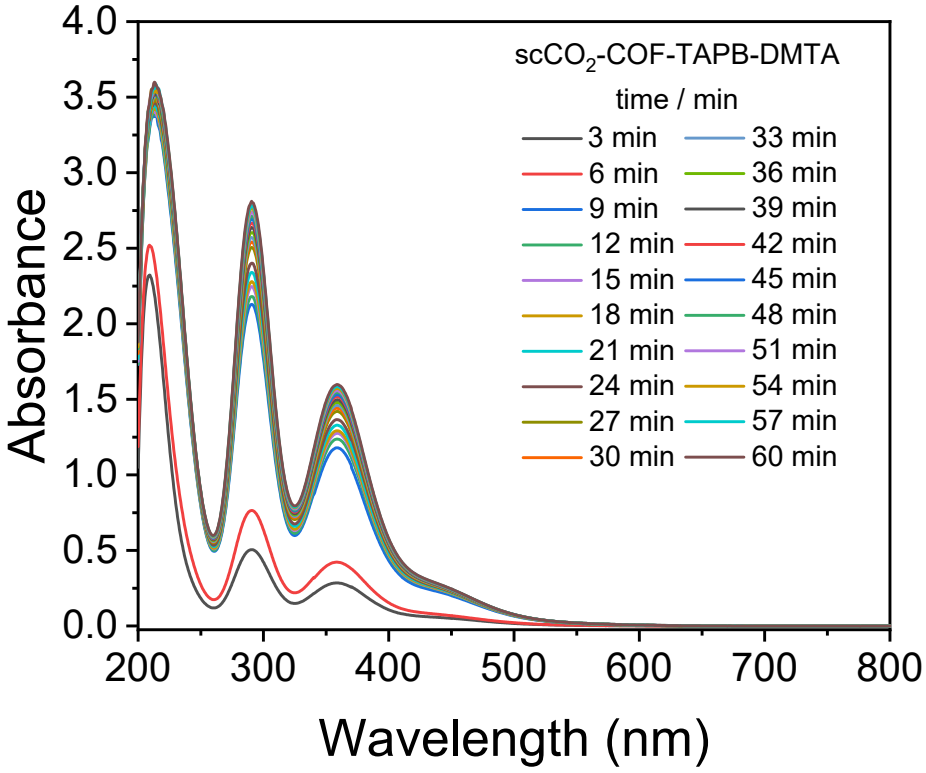

Figure S13a. Temporal evolution of UV-vis absorption spectra for the delivery of iodine from I_2@$scCO_2$-COF-TAPB-DMTA.

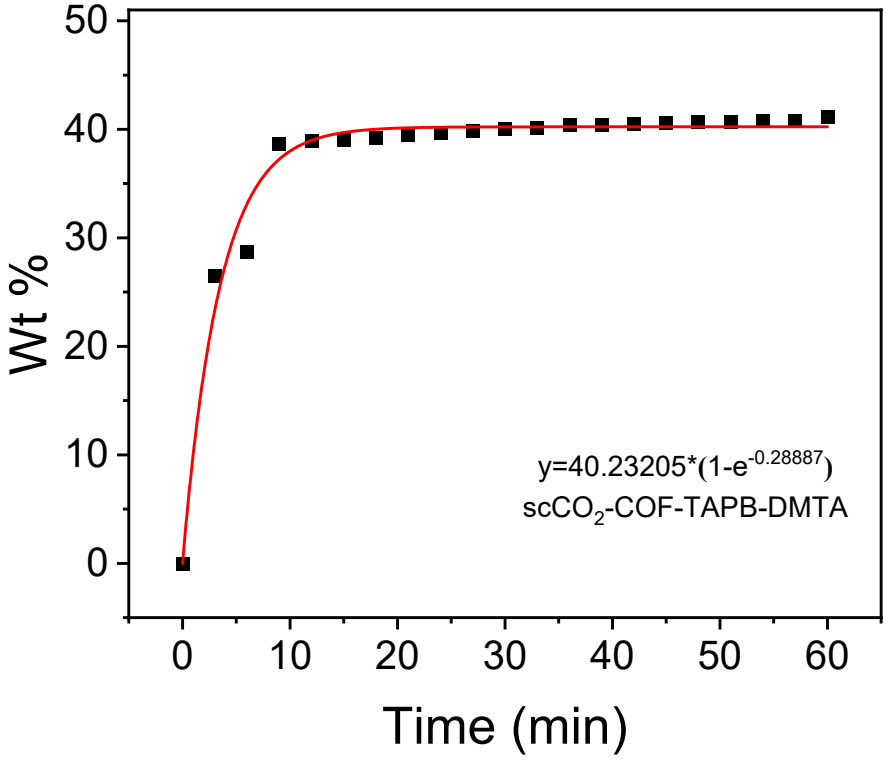

Figure S13b. The release of iodine from I_2@$scCO_2$-COF-TAPB-DMTA.

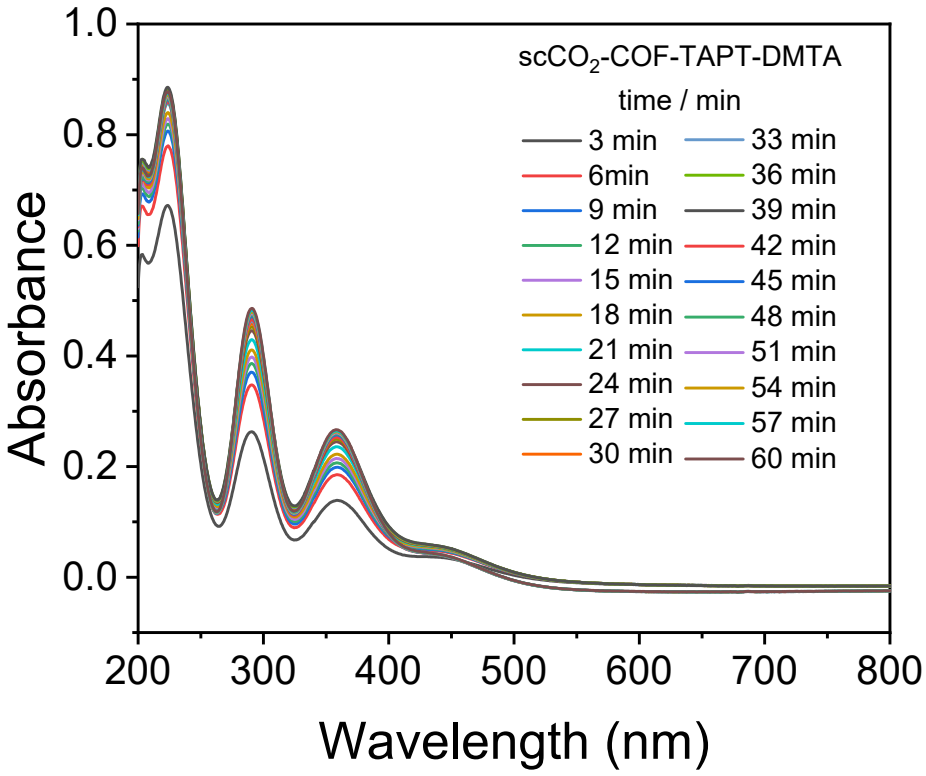

Figure S14a. Temporal evolution of UV-vis absorption spectra for the delivery of iodine from I_2@$scCO_2$-COF-TAPT-DMTA.

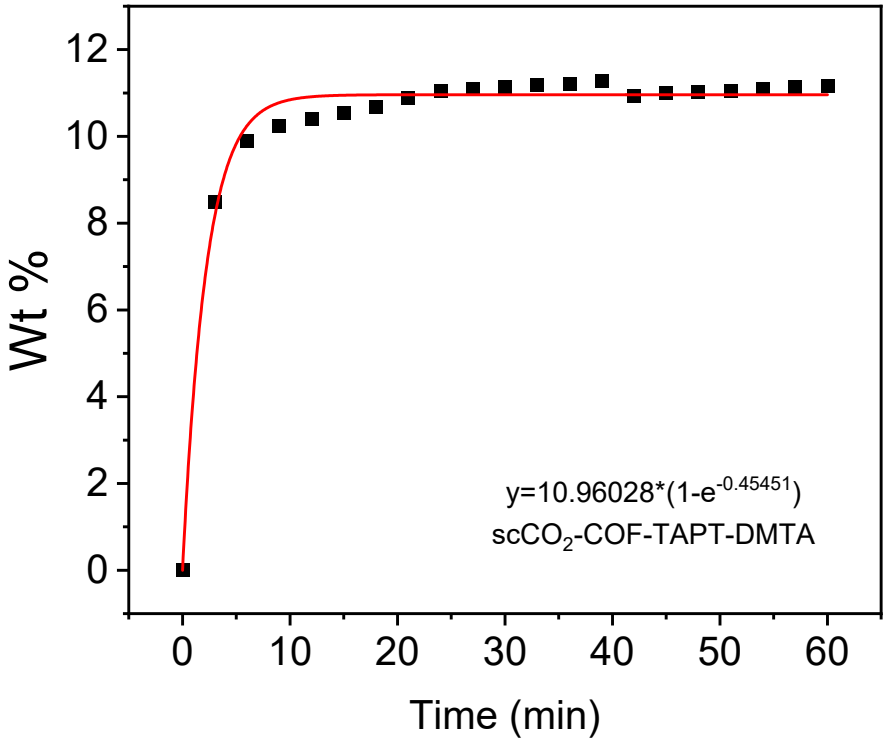

Figure S14b. The release of iodine from I_2@$scCO_2$-COF-TAPT-DMTA.

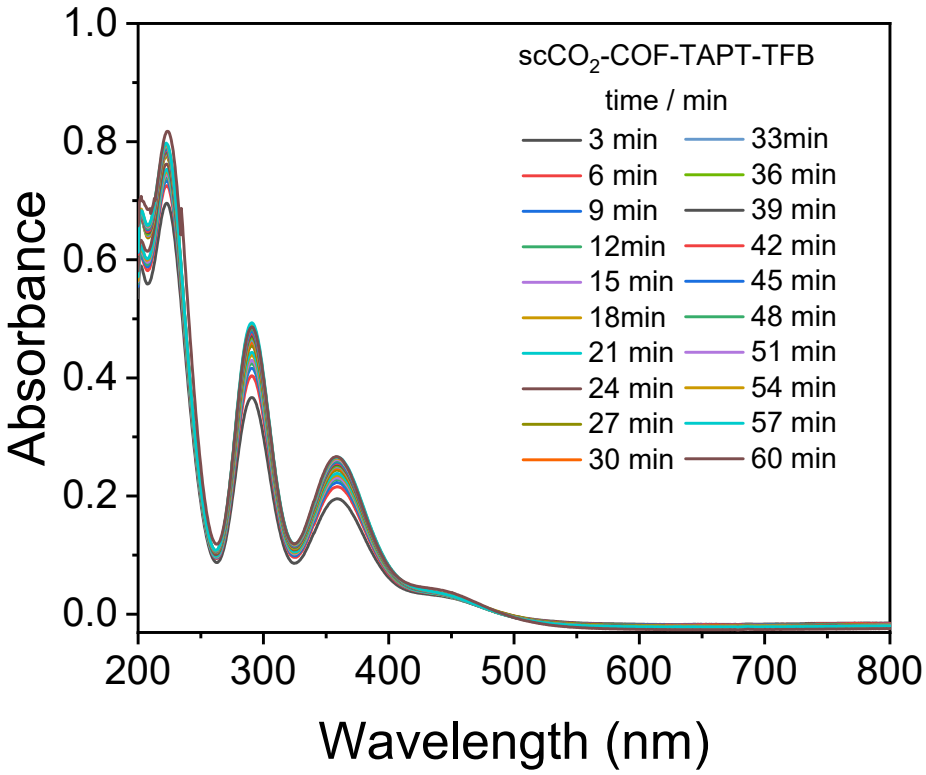

Figure S15a. Temporal evolution of UV-vis absorption spectra for the delivery of iodine from I_2@scCO_2-COF-TAPT-TFB.

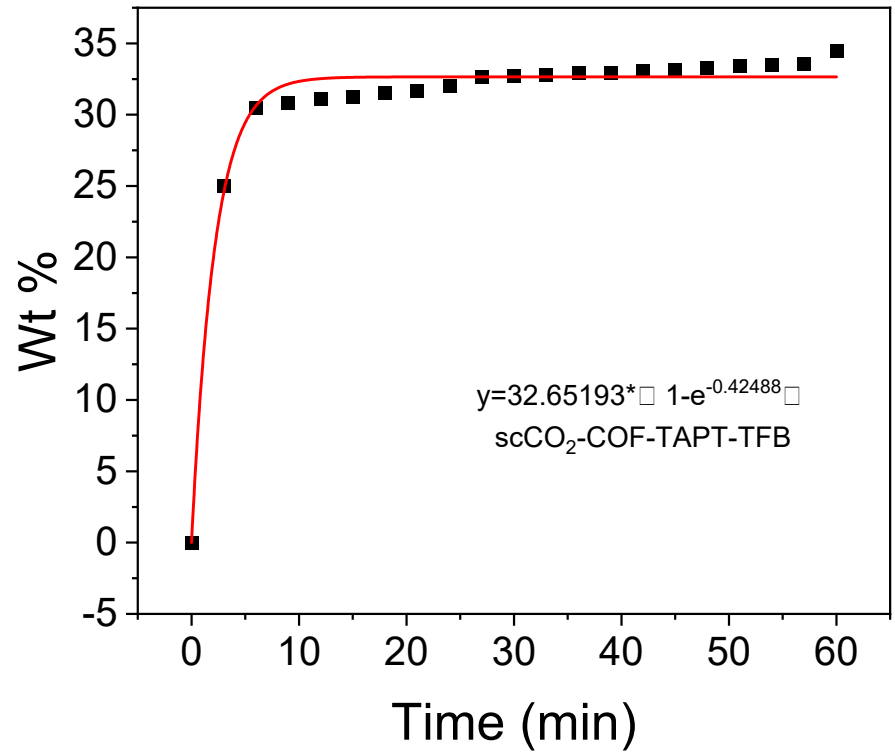

Figure S15b. The release of iodine from I_2@scCO_2-COF-TAPT-TFB.

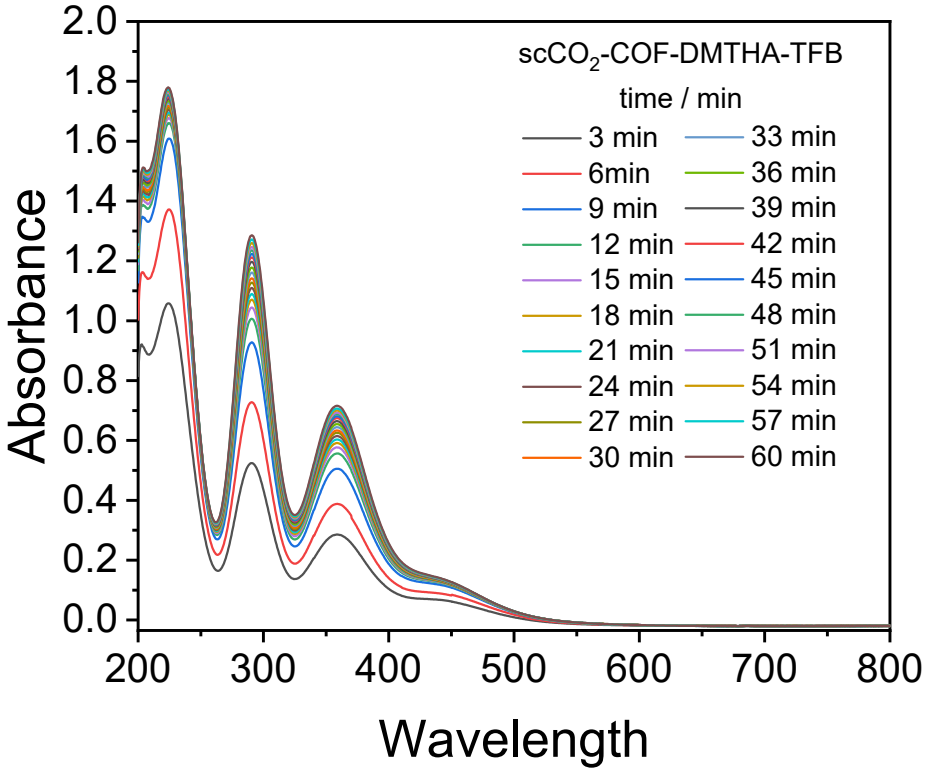

Figure S16a. Temporal evolution of UV-vis absorption spectra for the delivery of iodine from I_2@scCO_2-COF-DMTHA-TFB.

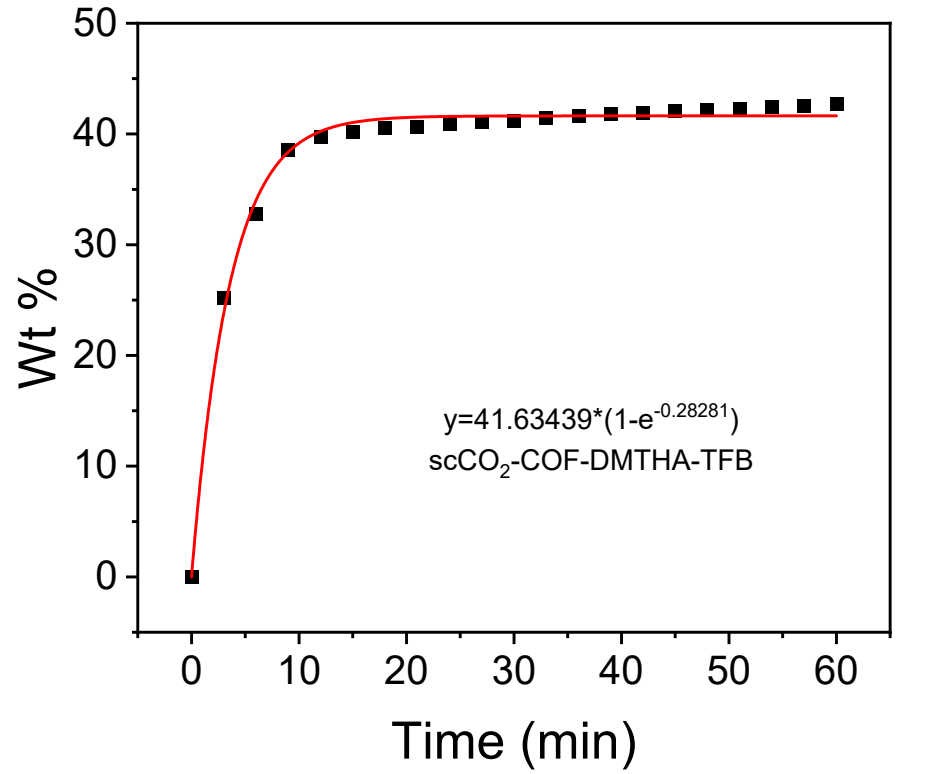

Figure S16b. The release of iodine from I_2@scCO_2-COF-DMTHA-TFB.

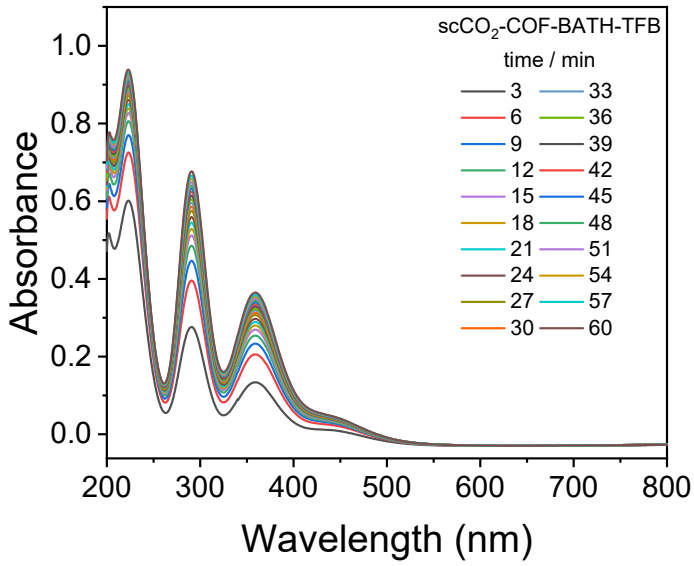

Figure S17a. Temporal evolution of UV-vis absorption spectra for the delivery of iodine from I_2@scCO$_2$-COF-BATH-TFB.

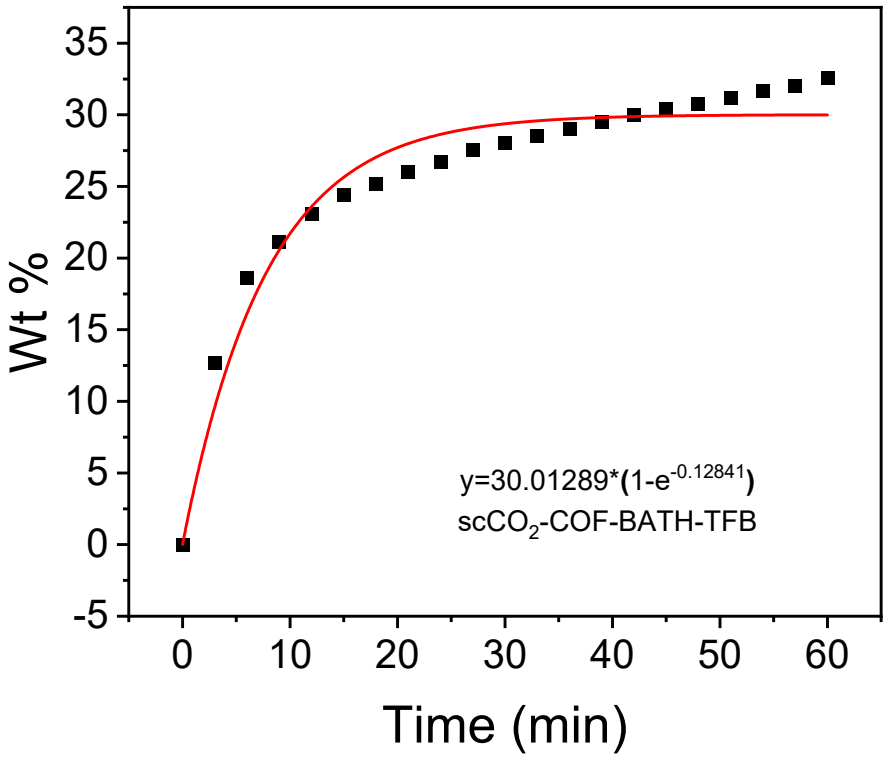

Figure S17b. The release of iodine from I_2@scCO$_2$-COF-BATH-TFB.

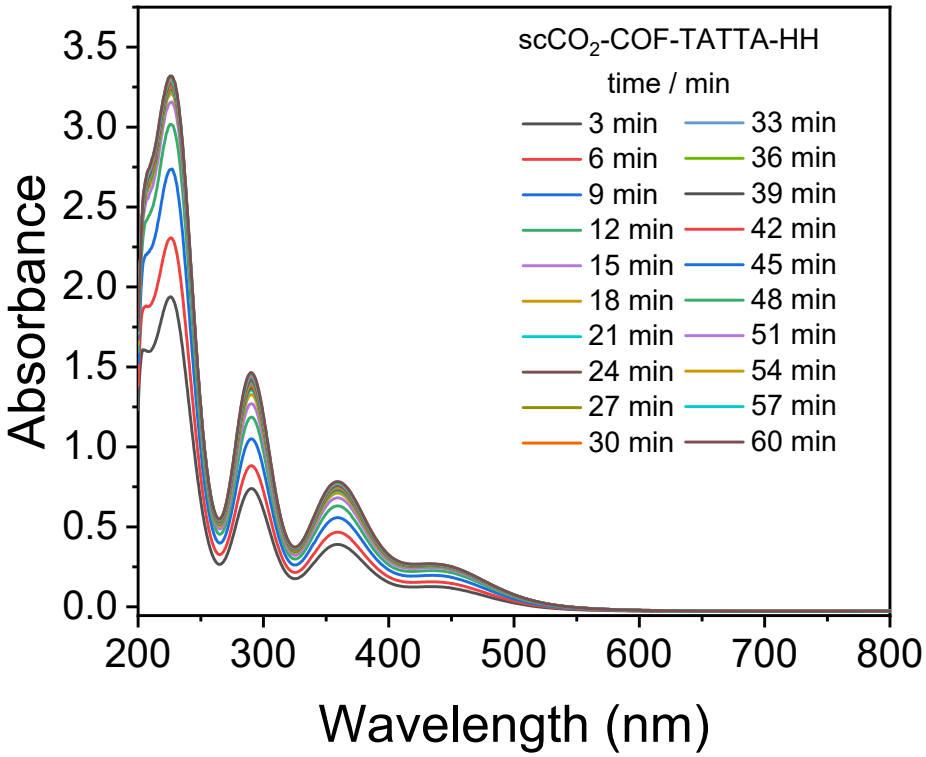

Figure S18a. Temporal evolution of UV-vis absorption spectra for the delivery of iodine from I_2@scCO$_2$-COF-TATTA-HH.

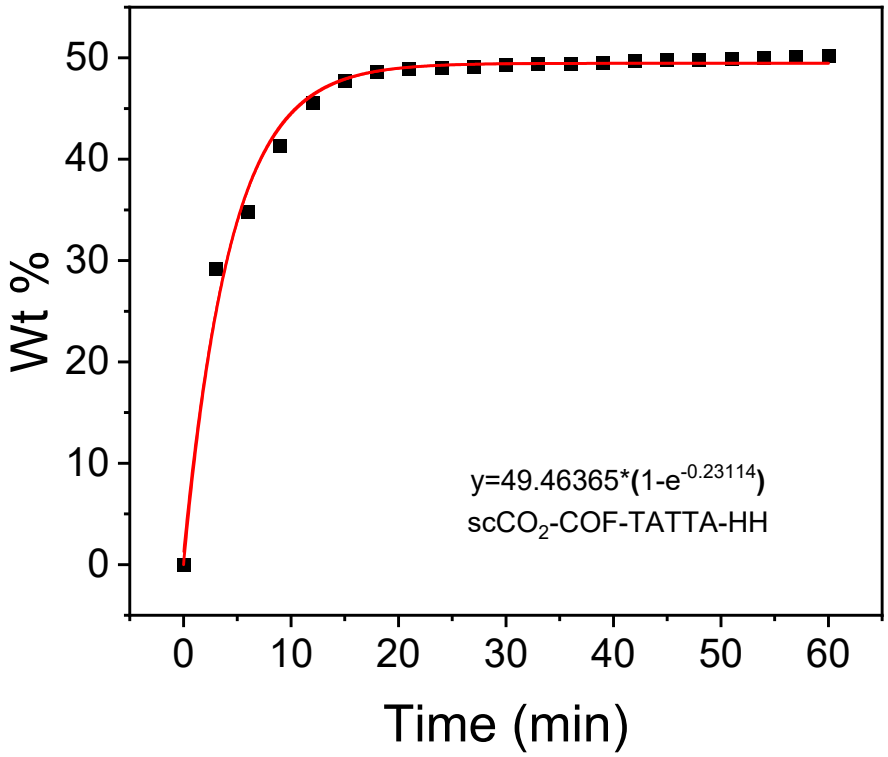

Figure S18b. The release of iodine from I_2@scCO$_2$-COF-TATTA-HH.

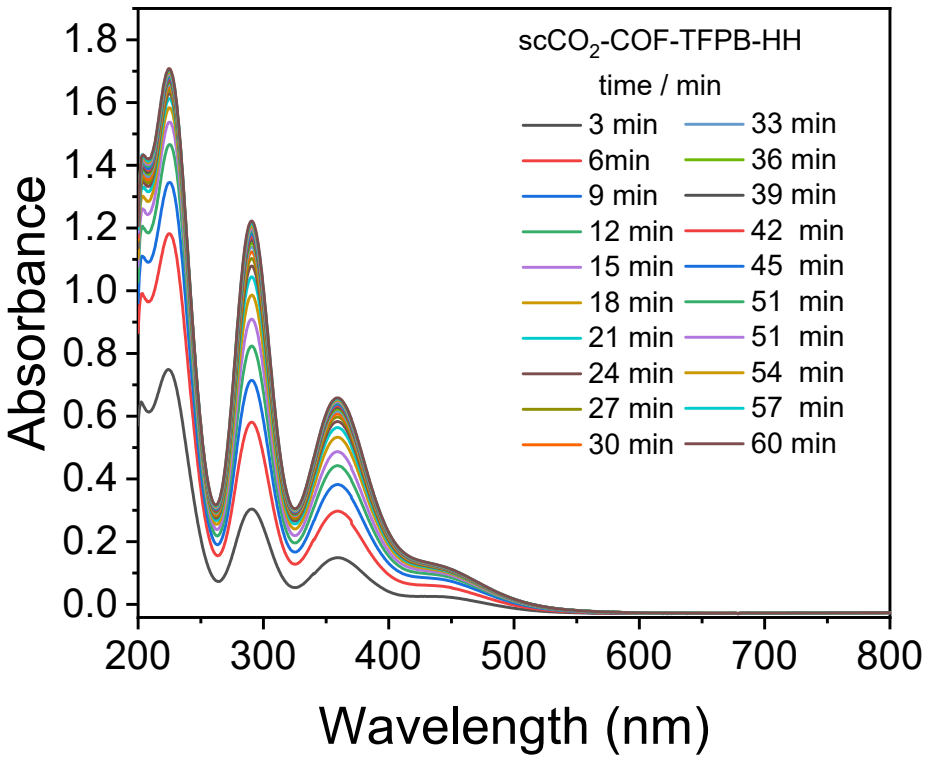

Figure S19a. Temporal evolution of UV-vis absorption spectra for the delivery of iodine from I_2@scCO_2-COF-TFPB-HH.

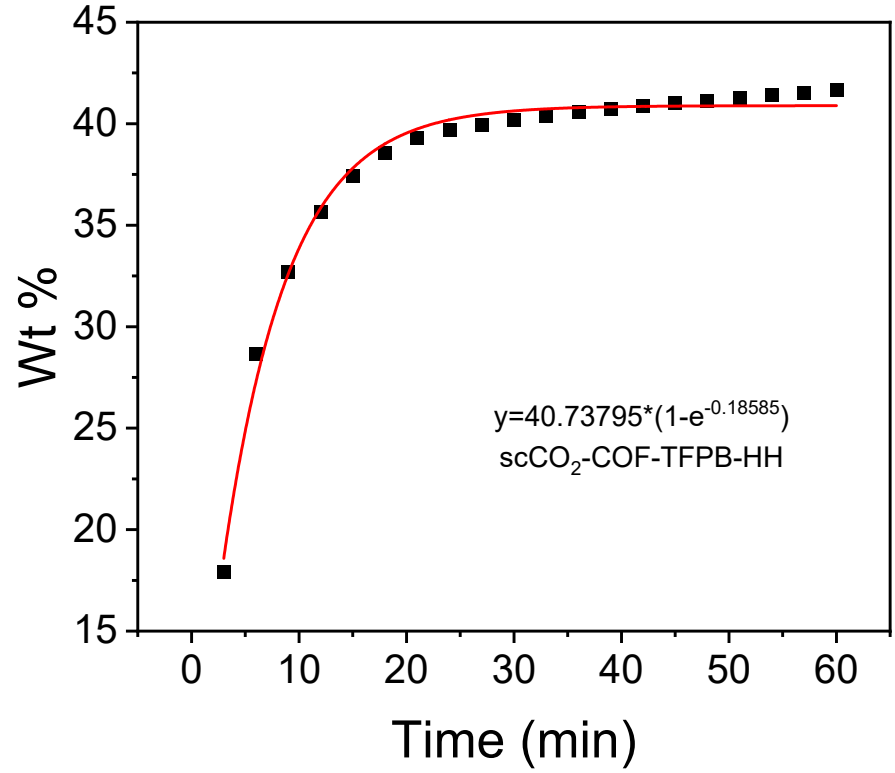

Figure S19b. The release of iodine from I_2@scCO_2-COF-TFPB-HH.

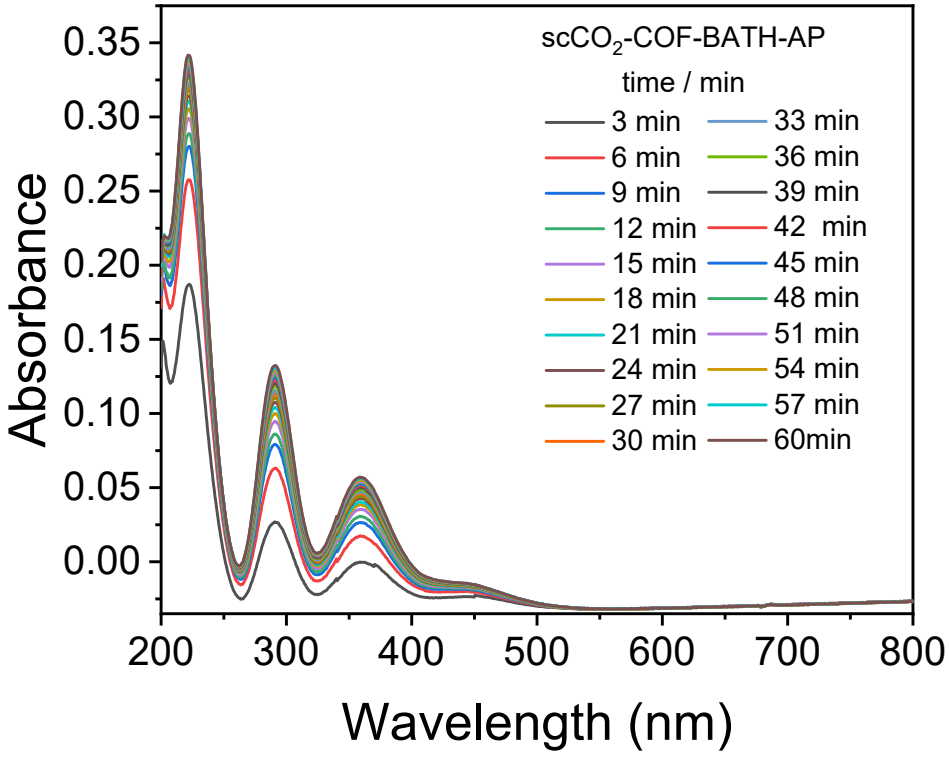

Figure S20a. Temporal evolution of UV-vis absorption spectra for the delivery of iodine from I_2@scCO$_2$-COF-BATH-AP.

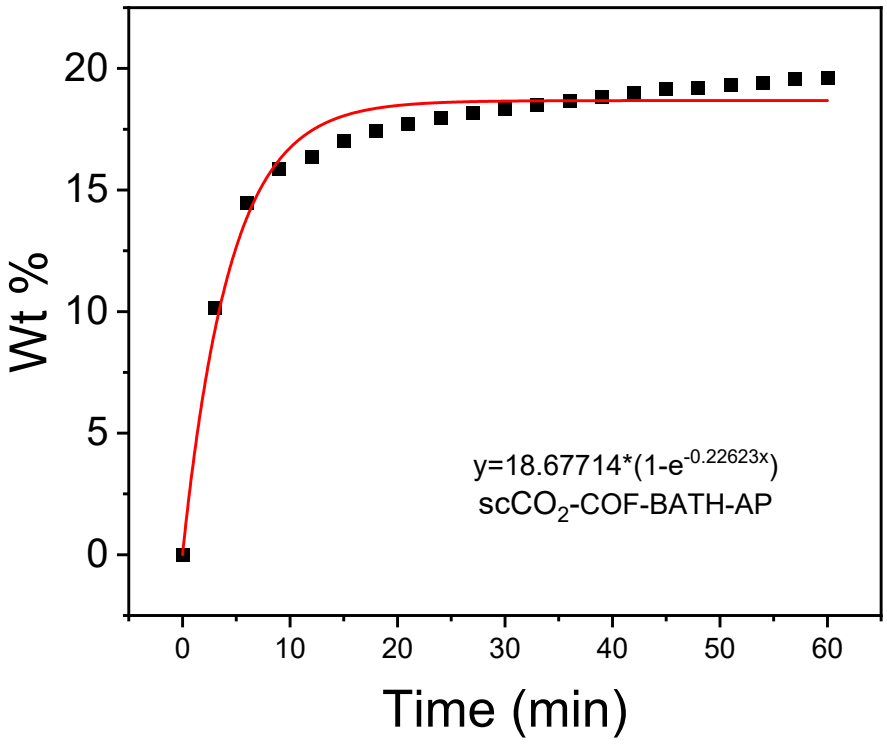

Figure S20b. The release of iodine from I_2@scCO$_2$-COF-BATH-AP.

References

1. B.-J. Yao, J.-T. Li, N. Huang, J.-L. Kan, L. Qiao, L.-G. Ding, F. Li and Y.-B. Dong, *ACS applied materials & interfaces*, 2018, **10**, 20448-20457.
2. H. Xu, J. Gao and D. Jiang, *Nature chemistry*, 2015, **7**, 905-912.
3. J. Yang, Y. Cao, W. Si, J. Zhang, J. Wang, Y. Qu and W. Qin, *ChemSusChem*, 2022, **15**, e202200100.
4. S. Yang, W. Hu, X. Zhang, P. He, B. Pattengale, C. Liu, M. Cendejas, I. Hermans, X. Zhang and J. Zhang, *Journal of the American Chemical Society*, 2018, **140**, 14614-14618.
5. X. Li, Q. Gao, J. Wang, Y. Chen, Z.-H. Chen, H.-S. Xu, W. Tang, K. Leng, G.-H. Ning and J. Wu, *Nature communications*, 2018, **9**, 2335.
6. X. Li, J. Qiao, S. W. Chee, H.-S. Xu, X. Zhao, H. S. Choi, W. Yu, S. Y. Quek, U. Mirsaidov and K. P. Loh, *Journal of the American Chemical Society*, 2020, **142**, 4932-4943.
7. Z. Li, J.-A. Wang, S. Ma, Z. Zhang, Y. Zhi, F. Zhang, H. Xia, G. Henkelman and X. Liu, *Applied Catalysis B: Environmental*, 2022, **310**, 121335.
8. Y. Zhang, T. Mao, L. Hao, T. Sun, T. Wang, P. Cheng, Y. Chen, Z. Wang and Z. Zhang, *Macromolecular Rapid Communications*, 2023, **44**, 2200722.
9. F. Zhang, H. Hao, X. Dong, X. Li and X. Lang, *Applied Catalysis B: Environmental*, 2022, **305**, 121027.